

AD-A157 959

Final Report
for the period
31 August 1984 to
4 March 1985

Modeling and Control of Flexible Structures

May 1985

Authors:
J. A. Burns
E. M. Cliff
R. M. Goff
H. J. Kelley
F. H. Lutze

Optimization Incorporated
29 High Meadow Drive
Blacksburg, VA 24060

K506-1
F04611-84-C-0032

Approved for Public Release

Distribution unlimited. The AFRPL Technical Services Office has reviewed this report, and it is releasable to the National Technical Information Service, where it will be available to the general public, including foreign nationals.

prepared for the: **Air Force
Rocket Propulsion
Laboratory**

Air Force Space Technology Center
Space Division, Air Force Systems Command
Edwards Air Force Base,
California 93523-5000

85 8 3 03 7

DTIC FILE COPY

NOTICE

When U.S. Government drawings, specifications, or other data are used for any purpose other than a definitely related government procurement operation, the government thereby incurs no responsibility nor any obligation whatsoever, and the fact that the government may have formulated, furnished, or in any way supplied the said drawings, specifications, or other data, is not to be regarded by implication or otherwise, or conveying any rights or permission to manufacture, use, or sell any patented invention that may in any way be related thereto.

FOREWORD

This report was prepared by Optimization, Incorporated, in fulfillment of contract number F04611-84-C-0032 with the Air Force Rocket Propulsion Laboratory (AFRPL), Edwards Air Force Base, Calif. Project manager for the AFRPL was Lt Eric Dale.

This technical report has been reviewed and is approved for publication and distribution in accordance with the distribution statement on the cover and on the DD Form 1473.

Eric M. Dale
ERIC M. DALE, 2Lt, USAF
Project Manager

L. Kevin Slimak
L. KEVIN SLIMAK
Chief, Interdisciplinary Space
Technology Branch

FOR THE DIRECTOR

Homer M. Pressley Jr.
HOMER M. PRESSLEY, Lt Col, USAF
Chief, Propulsion Analysis Division

Approval For	
1. CAA/1	<input checked="" type="checkbox"/>
2. TAB	<input type="checkbox"/>
3. General	<input type="checkbox"/>
4. Distribution	
5. Comments	
6. Remarks	
7. Date	

A-1

AD A 157 959

REPORT DOCUMENTATION PAGE

1a. REPORT SECURITY CLASSIFICATION UNCLASSIFIED			1b. RESTRICTIVE MARKINGS		
2a. SECURITY CLASSIFICATION AUTHORITY			3. DISTRIBUTION/AVAILABILITY OF REPORT PUBLIC RELEASE. DISTRIBUTION IS UNLIMITED.		
2b. DECLASSIFICATION/DOWNGRADING SCHEDULE					
4. PERFORMING ORGANIZATION REPORT NUMBER(S) K506-1			5. MONITORING ORGANIZATION REPORT NUMBER(S) AFRPL-TR-85-030		
6a. NAME OF PERFORMING ORGANIZATION Optimization Incorporated		6b. OFFICE SYMBOL (If applicable)		7a. NAME OF MONITORING ORGANIZATION Air Force Rocket Propulsion Laboratory	
6c. ADDRESS (City, State and ZIP Code) 29 High Meadow Drive Blacksburg, VA 24060				7b. ADDRESS (City, State and ZIP Code) AFRPL/DYSS, Stop 24 Edwards Air Force Base, CA 93523-5000	
8a. NAME OF FUNDING/SPONSORING ORGANIZATION		8b. OFFICE SYMBOL (If applicable)		9. PROCUREMENT INSTRUMENT IDENTIFICATION NUMBER F04611-84-C-0032	
8c. ADDRESS (City, State and ZIP Code)		10. SOURCE OF FUNDING NOS.			
		PROGRAM ELEMENT NO.		PROJECT NO.	TASK NO.
		62302F		2864	00
11. TITLE (Include Security Classification) MODELING AND CONTROL OF FLEXIBLE STRUCTURES (U)		12. PERSONAL AUTHOR(S) Burns, J. A., Cliff, E. M., Goff, R. M., Kelley, H. J., and Lutz, F. H.			
13a. TYPE OF REPORT Final		13b. TIME COVERED FROM 84/8/31 TO 85/3/4		14. DATE OF REPORT (Yr., Mo., Day) 85/5	
				15. PAGE COUNT 101	
16. SUPPLEMENTARY NOTATION					
17. COSATI CODES			18. SUBJECT TERMS (Continue on reverse if necessary and identify by block number)		
FIELD	GROUP	SUB. GR.	Distributed-Parameter Systems, Flexible Structures Control.		
22	02				
19. ABSTRACT (Continue on reverse if necessary and identify by block number)					
<p>The principal goals of this program were a demonstration of state-space procedure for modeling and control of a flexible structure, and, more generally, increased understanding of control problems for such systems. The state-space approach is based on a model of the distributed system. That is, the model includes the necessary partial differential equations without modal truncation. The basic view is that it is preferable to avoid introducing approximations until they are required (e.g., for numerical calculations). The program (formal modal, state-space model, optimal-control formulation, approximation procedure and numerical calculation) is carried out, in detail, for a simple structural system including a rotating hub, a flexible beam and a tip mass. The work is described in Part I of this report. A final section in this part provides some parallel results for a more complex structure comprised of a hub, two flexible support beams and a tip-body.</p> <p>The second part of the report is concerned with some parasitic effects on the stability of a distributed system with feedback. The approach is based on an input-output descrip-</p>					
20. DISTRIBUTION/AVAILABILITY OF ABSTRACT UNCLASSIFIED/UNLIMITED <input type="checkbox"/> SAME AS RPT. <input checked="" type="checkbox"/> DTIC USERS <input type="checkbox"/>			21. ABSTRACT SECURITY CLASSIFICATION UNCLASSIFIED		
22a. NAME OF RESPONSIBLE INDIVIDUAL Eric M. Dale, 2Lt, USAF		22b. TELEPHONE NUMBER (Include Area Code) (805) 277-5483		22c. OFFICE SYMBOL DYSS	

Block 19 (Continued):

tion of the system; specifically, a transfer-function approach is used. In order to keep the calculation burden reasonably small the structural model studied is a simple cable which requires only second-order spatial derivatives. The baseline system employs feed-back of a force to the "free end" of the cable at a magnitude proportional to the velocity at the "free end". The gain parameter can be varied to produce a locus of roots; albeit one with a countably infinite number of branches.

The basic system is examined and then the effects of three modifications are studied. These are: time-delay in the feed-back loop; time-lag in the feed-back loop; and, viscous damping in the system forward-loop. The most startling result is that with time-delay the undamped system will be unstable for any non-zero gain. Viscous damping apparently provides some help here; with such damping the system will be stable at least for "small" gain values.

TABLE OF CONTENTS

<u>Section</u>	<u>Page</u>
Overview	iv
PART I: STATE SPACE CONTROL OF A FLEXIBLE STRUCTURE	1
Introduction	1
Section I. Equations of Motion	3
Section II. State Space Formulation	12
Section III. The Control Problem	27
Section IV. Numerical Procedures	38
Section V. The Two-Beam Structure	48
REFERENCES FOR PART I	56
FIGURES FOR PART I	57
PART II: EFFECTS OF TIME DELAY, ACTUATOR DYNAMICS AND SYSTEM DAMPING ON THE FEEDBACK CONTROL OF A FLEXIBLE CABLE.	62
Section I. Introduction	63
Section II. Flexible Cable Analysis	64
Section III. Flexible Cable-Stability and Control	67
Section IV. Feedback Control with First Order Actuator	74
Section V. Feedback Control with System Damping	76
Section VI. Closure	79
REFERENCES FOR PART II	81
FIGURES FOR PART II	82
PROGRAM LISTING	92

OVERVIEW

This report summarizes work done under Contract F04611-84-C-0032 during the period 31 August 1984 through 1 March 1985. The principal goals were a demonstration of state-space procedure for modelling and control of a flexible structure, and, more generally, increased understanding of control problems for such systems. The state-space approach is based on a model of the distributed system. That is, the model includes the necessary partial differential equations without modal truncation. The basic view is that it is preferable to avoid introducing approximations until they are required (e.g., for numerical calculations). The program (formal model, state-space model, optimal-control formulation, approximation procedure and numerical calculation) is carried out, in detail, for a simple structural system including a rotating hub, a flexible beam and a tip mass. The work is described in Part I of this report. A final section in this Part provides some parallel results for a more complex structure comprised of a hub, two flexible support beams and a tip-body.

The second part of the report is concerned with some parasitic effects on the stability of a distributed system with feedback. The approach is based on an input-output description of the system; specifically, a transfer-function approach is used. In order to keep the calculation burden reasonably small the structural model studied is a simple cable which requires only second-order spatial derivatives. The baseline system employs feedback of a force to the "free end" of the

cable at a magnitude proportional to the velocity at the "free end".

The gain parameter can be varied to produce a locus of roots; albeit one with a countably infinite number of branches.

The basic system is examined and then the effects of three modifications are studied. These are: time-delay in the feed-back loop; time-lag in the feed-back loop; and, viscous damping in the system forward-loop. The most startling result is that with time-delay the undamped system will be unstable for any non-zero gain. Viscous damping apparently provides some help here; with such damping the system will be stable at least for "small" gain values.

INTRODUCTION

This report deals with modelling and control of the structure shown in Figure 1. It is assumed that the structure is pivoting about a fixed pivot at point 0, and that the motion is in a plane. The structure consists of three parts, the main frame (body A), the beam (body B), and the end mass (body C). The main frame is assumed to be a rigid body pivoting about point 0. The beam is assumed to be flexible and rigidly attached to the main frame as a cantilevered beam. Finally, the end mass is rigidly attached to the end of the beam so that it moves and rotates with the end of the beam and its attachment point is assumed to be at the center of mass of the end mass. A free body diagram of each mass is shown in Figure 2.

This report may be logically divided into five parts. In the next section a 'formal' model for the system is developed. This is done by a direct application of Newtonian mechanics to each of the structural components. The model is 'formal' in the sense that no attempt is made to show that the resulting system of (coupled partial and ordinary) differential equations is well-posed. That is, we do not prove that the system has a unique solution for a certain class of initial data, nor do we prove that the solution depends continuously on the initial data.

A second section is concerned with development of an abstract state-space model. Since the differential equations are linear (more appropriately linearized), the abstract model is in the form

$$\dot{y}(t) = Ay(t) + Bu(t)$$

where $y(t)$ is the state at time t , $u(t)$ is the control and A and B are linear operators. The point of this formulation is that one has a theory that guarantees well-posedness under concrete and verifiable conditions on the operators. We construct our model so that the system has these properties and hence we have a guarantee that the differential system makes sense.

A third section is devoted to linear-quadratic regulator theory for the abstract system. The feedback structure of the optimal control is discussed along with a factorization procedure that can significantly reduce the computational problem. A general theory of numerical approximation is also included in this section. A fourth section presents details for developing a class of numerical approximations. Some numerical results are included.

The final section describes an analysis of a more complex structure including a rigid hub, two flexible side beams and a tip-body. This analysis parallels that of the simpler case but provides fewer details and no numerical results.

I. EQUATIONS OF MOTION

The mathematical model of the structure shown in Figure 1 is developed in this section. It is assumed that the structure is pivoting about a fixed pivot at point 0, and that the motion is in a plane. The development is achieved by direct application of Newton's Laws to individual members of the structure with the resulting equations summed to determine the overall motion. The development is rigorous with assumptions stated as needed or desired.

The structure consists of three parts, the main frame, or mass A, the beam, or mass B, and the end mass, or mass C. The main frame is assumed to be a rigid body pivoting about point 0. The beam is assumed to be flexible and rigidly attached to the main frame as a cantilevered beam. The end mass is rigidly attached to the end of the beam so that it moves and rotates with the end of the beam. Finally, the attached point is assumed to be at the center of mass of the end mass. A free body diagram of each mass is shown in Figure 2.

Beam Equations

The coordinate system to be used is fixed in the main frame and rotates with it. The origin is at point 0 with the x axis pointing along the undeflected beam, the z axis, the axis of rotation, and the y axis completing the right hand set. The position vector to some point on the beam is given by

$$\vec{r}(t,x) = \vec{r}(x) + \vec{u}(t,x) \quad (1.1)$$

where

$\vec{r}(x)$ = position to undeflected location of mass element dm

$\vec{u}(t,x)$ = position of mass element dm with respect to its undeflected position.

It is assumed here that the deflections \vec{u} are small. The governing equations are given by

$$\vec{r}(t,x) = \vec{r}(x) + \vec{u}(t,x)$$

$$\dot{\vec{r}}_{rel}(t,x) = \frac{\partial \vec{u}(t,x)}{\partial t} = \vec{u}_t(t,x) \quad (1.2)$$

$$\ddot{\vec{r}}_{rel}(t,x) = \frac{\partial^2 \vec{u}(t,x)}{\partial t^2} = \vec{u}_{tt}(t,x)$$

where

$\dot{\vec{r}}_{rel}(t,x)$ = velocity relative to the rotating coordinate system

$\ddot{\vec{r}}_{rel}(t,x)$ = acceleration relative to the rotating coordinate system

and by Newton's Laws which are [6]:

$$\vec{F} = \int_m \vec{a} \, dm$$

$$\vec{M}_0 = \int_m \vec{r} \times \vec{a} \, dm \quad (1.3)$$

where

\bar{F} = total external force

\bar{M}_0 = total external moment acting about point 0.

The general expression for the acceleration at any point is given by [6]

$$\bar{a} = \bar{a}_0 + \bar{\omega} \times (\bar{\omega} \times \bar{r}) + \dot{\bar{\omega}} \times \bar{r} + 2\bar{\omega} \times \dot{\bar{r}}_{\text{rel}} + \ddot{\bar{r}}_{\text{rel}} \quad (1.4)$$

We can note that for the conditions of this problem $\bar{a}_0 = 0$ since it is a fixed pivot.

We can apply the moment equation (1.3) to the beam. Substituting the expressions for \bar{r} and its derivatives (eq. 1.2) along with the expression for the acceleration (eq. 1.4) into (eq. 1.3) yields the general result:

$$\begin{aligned} \bar{M}_0^{(B)} = \int_m (\hat{r} \times [\bar{\omega} \times (\bar{\omega} \times \hat{r})] + \bar{u} \times [\bar{\omega} \times (\bar{\omega} \times \hat{r})] + \hat{r} \times [\bar{\omega} \times (\bar{\omega} \times \bar{u})] + \bar{u} \times [\bar{\omega} \times (\bar{\omega} \times \bar{u})] + \hat{r} \times (\dot{\bar{\omega}} \times \hat{r}) + \bar{u} \times (\dot{\bar{\omega}} \times \bar{r}) + \bar{u} \times (\dot{\bar{\omega}} \times \bar{u}) + \hat{r} \times (\dot{\bar{\omega}} \times \bar{u}) + 2\hat{r} \times (\bar{\omega} \times \bar{u}_t) + 2\bar{u} \times (\bar{\omega} \times \bar{u}_t) + \hat{r} \times \bar{u}_{tt} + \bar{u} \times \bar{u}_{tt}) \cdot d\mathbf{m} \end{aligned} \quad (1.5)$$

where $\bar{M}_0^{(B)}$ is the total applied moment on the beam about point 0.

Equation (1.5) reduces considerably if we take advantage of some additional assumptions. If ϵ is assumed small so that products such as ϵ^2 , ϵu and of course u^2 are negligible, all but two terms are dropped

from eq. (1.5). If we further assume the deflections occur only perpendicular to the beam (no stretching of the beam, consistent with small angular rates and deflections), then $\bar{u} = u\hat{j}$, and eq. (1.5) becomes

$$\bar{M}_0^{(B)} = (I_{OB}\dot{\omega}(t) + \int_m \hat{r} \times u_{tt}(t,x) dm) \hat{k} \quad (1.6)$$

where

$$I_{OB}\dot{\omega} = \int_m \hat{r} \times (\dot{\omega} \times \hat{r}) dm$$

I_{OB} = moment of inertia of the undeflected beam about point O.

Equation (1.6) is the beam moment equation.

The elastic equation for the beam is obtained from basic principles. If the beam is assumed to have uniform properties along its length, and that no external forces act on the beam except those at the boundaries, then the equation of motion of an element of the beam is given by [5]

$$\bar{a}(t,x) = - \frac{EI}{\rho} \frac{\partial^4 u(t,x)}{\partial x^4} \hat{j} = - \frac{EI}{\rho} u_{xxxx}(t,x) \hat{j} \quad (1.7)$$

where

EI = the stiffness properties of the beam (constant)

ρ = density per unit length of the beam (constant)

$\bar{a}(t,x)$ = the acceleration of the beam element.

The acceleration is given by eq. (1.4) which can be substituted into eq. (1.7). Under the previous assumptions, eq. (1.7) reduces to

$$u_{tt}(t,x) = - \frac{EI}{\rho} u_{xxxx}(t,x) - \dot{\omega}(t) \quad (1.8)$$

Main Frame

The equations for the main frame are similar to the rigid body equations of motion. The moment equation is

$$\bar{M}_0^{(A)} = I_A \ddot{\omega}(t) = I_A \dot{\omega}(t) \hat{k} \quad (1.9)$$

where

I_A = moment of inertia of main frame about point 0.

End Mass

Both the force and moment equations are needed for the end mass since it is translating as well as rotating. The force equation is given by

$$\bar{F}_C = \bar{F}_L = m_C \ddot{\bar{r}}(t, L) \quad (1.10)$$

where

\bar{F}_L = force on mass due to beam.

Under the previous assumptions, eq. (1.10) becomes

$$\begin{aligned} \bar{F}_L &= f_{Ly} \hat{j} \\ f_{Ly} &= m_C [L \ddot{x}(t) + \dot{v}_1(t)] \end{aligned} \quad (1.11)$$

where $v_1(t) = u_t(t, L)$, the relative velocity of the end of the beam (see eq. 1.2).

For planar motion, only the z component of the moment is of interest and leads to

$$M_c = I_c \ddot{\phi}(t) \quad (1.12)$$

where

I_c = moment of inertia of the end mass about its center of mass

$\phi(t)$ = the angular position of the end mass with respect to an inertial reference.

The angular position of the end mass is that due to the rigid body motion of the beam, (θ) , plus the angular motion due to the deflection of the beam which is equal to the slope of the beam,

$$\begin{aligned} \phi(t) &= \theta(t) + u_x(t, L) \\ \dot{\phi}(t) &= \dot{\theta}(t) + \dot{\zeta}(t) \\ \ddot{\phi}(t) &= \ddot{\theta}(t) + \ddot{\xi}(t) \end{aligned} \quad (1.13)$$

where

$\xi(t) = u_{xt}(t, L)$, the angular rate of the beam end due to deflection.

Consequently the moment equation can be written as

$$M_c = I_c [\ddot{\theta}(t) + \ddot{\xi}(t)] \quad (1.14)$$

System Moment Equation

The moment equation for the complete system can be obtained by combining the moment equations for each individual mass. In order to carry out this step it is necessary to write the expressions for the applied moments on the main frame and on the beam. These are respectively (see Figure 2)

$$M_0^{(A)} = M_A - M_{OB} \quad (1.15)$$

and

$$M_0^{(B)} = M_{OB} - M_C - Lf_{Ly} \quad (1.16)$$

By adding all the moment equations (1.6, 1.9 and 1.14) together and utilizing eqs. (1.11, 1.15 and 1.16) the system moment equation can be obtained. The result is

$$M_A = (I_A + I_{OB} + I_C + m_c L^2) \ddot{\omega}(t) + I_C \ddot{\xi}(t) + m_c L \ddot{\eta}(t) + \int_0^L x u_{tt}(t, x) dx \quad (1.17)$$

where the relation $dm = \rho dx$ has been used.

Boundary Conditions

Associated with the structural equation (1.8) are the following boundary conditions: (see Figure 2)

At $x = 0$

$$\left. \begin{aligned} u(t,0) &= 0 \\ u_x(t,0) &= 0 \end{aligned} \right\} \text{cantilever moment to mainframe} \quad (1.18)$$

$$u_x(t,0) = 0 \quad (1.19)$$

$$M_{OB} = -EI u_{xx}(t,0) \quad (1.20)$$

At $x = L$

$$u_t(t,L) = \eta(t) \quad (1.21)$$

$$u_{tx}(t,L) = \xi(t) \quad (1.22)$$

$$EI u_{xx}(t,L) = -M_c \quad (1.23)$$

$$f_{Ly} = EI u_{xxx}(t,L) \quad (1.24)$$

Final Working Equations

For the analysis which follows in the next section, it is useful to rearrange the equations developed previously into a final working set.

We have the structural equation (1.8)

$$u_{tt}(t,x) + \frac{\dot{x}(t)}{c} = -\frac{EI}{c} u_{xxxx}(t,x). \quad (1.25)$$

From the main frame moment equation (1.9), eq. (1.15) and the boundary condition (1.20) we obtain

$$I_A \ddot{\omega}(t) = -EI u_{xx}(t,0) + M_A(t) \quad (1.26)$$

The end mass force and moment equations (1.11 and 1.14 respectively) in conjunction with the boundary conditions (1.23) and 1.24) become

$$I_C [\ddot{\omega}(t) + \ddot{\xi}(t)] = EI u_{xx}(t,L) \quad (1.27)$$

and

$$m_C [L\ddot{\omega}(t) + \ddot{\eta}(t)] = EI u_{xxx}(t,L) \quad (1.28)$$

Equations (1.25-1.28) plus the remaining boundary conditions, eqs. (1.18, 1.19, 1.21 and 1.22) are the starting point for the analysis in the next sections.

II. STATE-SPACE FORMULATION

The purpose of this section is to construct a state-space model for the system dynamics. That is, we are seeking an appropriate state-space Y so that the (linearized) equations can be written as

$$\dot{y}(t) = Ay(t) + Bf(t) \quad (2.1)$$

where f is the control and A and B are appropriate operators. In addition we shall show that the operators A and B are sufficiently "nice" that the system (2.1) is well-posed. This means that for appropriate initial data $[y(0)]$ and control input f , the system (2.11) has a unique solution and that solution depends continuously on the initial data.

The formal modelling procedure of the previous section resulted in the following description:

$$u_{tt}(t,x) + x\dot{\omega}(t) = -\frac{EI}{D} u_{xxxx}(t,x) \quad (2.2)$$

$$I_A \dot{\omega}(t) = EI u_{xx}(t,0) + M_A(t) \quad (2.3)$$

$$I_C [\dot{\omega}(t) + \dot{\xi}(t)] = -EI u_{xx}(t,L) \quad (2.4)$$

$$m_C [L\dot{\omega}(t) + \dot{\eta}(t)] = EI u_{xxx}(t,L) \quad (2.5)$$

In addition to these differential equations there are important boundary conditions. Since the beam remains joined to the hub one has

$$u(t,0) = u_t(t,0) = 0 \quad .$$

The cantilever nature of the connection also requires that

$$u_x(t,0) = u_{xt}(t,0) = 0 \quad ,$$

while integrity of the upper joint requires

$$u_t(t,L) = n(t) \quad ,$$

and

$$u_{xt}(t,L) = \xi(t) \quad .$$

As a first step in the state-space formulation observe that the partial differential equation (2.2) can be re-cast as a first-order system.

$$\frac{\partial}{\partial t} [u_{xx}(t,x)] = \frac{\partial^2}{\partial x^2} [u_t(t,x) + x \cdot \omega(t)] \quad (2.6)$$

$$\frac{\partial}{\partial t} [u_t(t,x) + x \cdot \omega(t)] = -\frac{EI}{S} \frac{\partial^2}{\partial x^2} [u_{xx}(t,x)]$$

This suggests that the functions (of x) $[u_{xx}(t,x)]$ and $[u_t(t,x) + x\omega(t)]$ are worthy of consideration as state components. With this insight define a "state" $z(t)$ by

$$z(t) = \begin{bmatrix} \omega(t) \\ \eta(t) \\ \xi(t) \\ u_{xx}(t,x) \\ u_t(t,x) + x\omega(t) \end{bmatrix}$$

Note that $z(t)$ has five coordinates:

ω	angular velocity of the hub
η	relative lineal velocity of the tip
ξ	relative angular velocity of the tip
u_{xx}	curvature of the beam
$u_t + x\omega$	velocity of the beam

The quantities ω , η and ξ are each scalar while $[u_{xx}]$ and $[u_t + x\omega]$ are functions of the spatial variable x . Thus, the state-space can be at least formally identified as

$$Z = R \times R \times R \times L_2 \times L_2$$

where R denotes the real line and L_2 is the usual Lebesgue space of real-valued, square-integrable 'functions' defined on the interval $[0,L]$ (see [9]).

It is possible to re-write the equations (2.2) - (2.5) in terms of the five components of Z and the control M_A .

$$\begin{aligned}
 I_A \dot{z}_1(t) &= EI \varepsilon_0 z_4(t) + M_A(t) \\
 m_c [L \dot{z}_1(t) + \dot{z}_2(t)] &= EI \varepsilon_L \circ D z_4(t) \\
 I_c [\dot{z}_1(t) + \dot{z}_3(t)] &= EI \varepsilon_L z_4(t) \\
 \dot{z}_4(t) &= D^2 z_5(t) \\
 \dot{z}_5(t) &= \frac{-EI}{\rho} D^2 z_4(t)
 \end{aligned} \tag{2.7}$$

In these equations D denotes differentiation with respect to the spatial variable x and ε_b denotes evaluation at $x = b$. Boundary conditions require that

$$\begin{aligned}
 \varepsilon_0 z_5(t) &= u_t(t, 0) = 0, \\
 \varepsilon_L z_5(t) &= u_t(t, L) + L\omega(t) \\
 &= n(t) + L\omega(t) \\
 &= z_2(t) + L z_1(t), \\
 \varepsilon_0 \circ D z_5(t) &= u_{tx}(t, 0) = 0,
 \end{aligned}$$

and

$$\begin{aligned} E_L \circ DZ_5(t) &= u_{tx}(t, L) + \omega(t) \cdot L \\ &= z_3(t) + z_1(t) \cdot L. \end{aligned}$$

The system (2.7) is in the form

$$F\dot{z}(t) = Gz(t) + Hf(t).$$

In principle, this can be brought into the normal form (2.1) by 'inverting' F . It is, perhaps, somewhat easier to introduce a coordinate transformation that 'uncouples' the left hand side.

Let $y_i = z_i$ ($i = 1, 4$ and 6) while $y_2 = Lz_1 + z_2$ and $y_3 = z_1 + z_3$. It may be verified that the system (2.7) can be written in the form (2.1) with

$$A = \begin{bmatrix} 0 & 0 & 0 & \frac{EI}{I_A} E_0 & 0 \\ 0 & 0 & 0 & \frac{EI}{m_c} E_L \circ D & 0 \\ 0 & 0 & 0 & -\frac{EI}{I_c} E_L & 0 \\ 0 & 0 & 0 & 0 & D^2 \\ 0 & 0 & 0 & -\frac{EI}{c} D^2 & 0 \end{bmatrix} \quad (2.8)$$

and

$$B = \begin{bmatrix} \frac{1}{T_A} \\ 0 \\ 0 \\ 0 \\ 0 \end{bmatrix} \quad (2.9)$$

The boundary conditions are readily translated to

$$\begin{aligned} E_0 y_5(t) &= 0 \\ E_L y_5(t) &= y_2(t) \\ E_0 \circ D y_5(t) &= 0 \\ E_L \circ D y_5(t) &= y_3(t) \end{aligned}$$

These conditions are incorporated by restricting the domain of the operator A to

$$\begin{aligned} D(A) &= \{(y_1, y_2, y_3, y_4, y_5) \in R^3 \times L_2 \times L_2 \mid \\ & y_4, y_5 \in W^{2,2}, y_5(0) = 0, y_5(L) = y_2 \\ & y_5'(0) = 0, y_5'(L) = y_3\}. \end{aligned} \quad (2.10)$$

$W^{2,2}$ is the usual space of real-valued functions with the function and its derivative in $L_2[1]$. As a distance measure on the space Y we introduce the inner-product

$$\begin{aligned} \langle y, w \rangle = & \frac{1}{2} I_A y_1 w_1 + \frac{1}{2} m_c y_2 w_2 + \frac{1}{2} I_c y_3 w_3 \\ & + \int_0^L EI y_4(x) w_4(x) dx + \int_0^L c y_5(x) w_5(x) dx \end{aligned} \quad (2.11)$$

It can be verified that $\|y\| = \sqrt{\langle y, y \rangle}$ is a norm and that Y is a Hilbert space. The inner-product $\langle y, y \rangle$ is the mechanical energy in the physical system at state y .

At this point we have constructed a system

$$\dot{y}(t) = Ay(t) + Bf(t) \quad (2.1)$$

with state-space $Y = \mathbb{R}^3 \times L_2 \times L_2$, inner product $\langle \cdot, \cdot \rangle$ [given by (2.11)] and operators A and B [given by (2.8), (2.9) and (2.10)]. The final part of this section is concerned with establishing that this system makes sense. Formally one can write down the solution to (2.1) in terms of the variation of constants formula

$$y(t) = e^{At} y(0) + \int_0^t e^{A(t-s)} B f(s) ds$$

Since B is bounded, the solution y will have the desired properties (existence, uniqueness and continuous dependence on initial data) if, and only if, e^{At} is a C_0 -semigroup. Hence, we must show that an A operator "generates" such a semigroup. This is the central matter in abstract formulations such as (2.1).

Over the last thirty-five years there has been significant progress in characterizing those operators that are generators of semigroups

[4,7,12]. We shall make use of a special form of the Lumer-Phillips Theorem [7].

Theorem (Lumer-Phillips): Let A be a densely defined, closed linear operator. If both A and A^* are dissipative, then A is the generator of a C_0 semigroup of contractions on Y .

To employ this theorem we must demonstrate that the A defined by (2.8, 2.10) satisfies the hypothesis. The fact that A is closed and densely defined follows from standard results in L_2 theory [9].

Lemma 2.1: The operator A constructed above is dissipative.

Proof: We must show that $\langle y, Ay \rangle \leq 0$ for all $y \in D(A)$.

Direct calculation reveals that

$$\begin{aligned} \langle y, y \rangle &= \frac{1}{2} I_A y_1 \frac{EI}{I_A} y_4'(0) \\ &\quad + \frac{1}{2} m_c y_2 \frac{EI}{m_c} y_4'(L) \\ &\quad + \frac{1}{2} I_c y_3 \frac{(-EI)}{I_c} y_4'(L) \\ &\quad + \frac{1}{2} EI \int_0^L y_4(x) y_5''(x) dx \\ &\quad + \frac{1}{2} \int_0^L y_5(x) \frac{(-EI)}{I_c} y_4''(x) dx \end{aligned}$$

After elementary calculations it is seen that each term has a common factor ($\frac{1}{2} EI$). The last two terms are each integrated by parts to produce

$$\begin{aligned} \frac{2\langle y, Ay \rangle}{EI} &= y_1 y_4(0) + y_2 y_4'(L) - y_3 y_4(L) \\ &\quad + (y_4(L) y_5'(L) - y_4(0) y_5'(0) - \int_0^L y_4'(x) y_5'(x) dx) \\ &\quad - (y_5(L) y_4'(L) - y_5(0) y_4'(0) - \int_0^L y_5'(x) y_4'(x) dx) . \end{aligned}$$

The integral terms cancel and the remaining terms can be gathered to yield

$$\begin{aligned} \frac{2\langle y, Ay \rangle}{EI} &= y_4(0)[y_1 - y_5'(0)] + y_4'(L)[y_2 - y_5(L)] \\ &\quad + y_4(L)[y_5'(L) - y_3] + y_4''(0)[y_5(0)] \end{aligned}$$

It is now easily verified that for y in the domain of [see (2.11)] each of the bracketed terms is zero so that

$$\langle y, Ay \rangle = 0 .$$

Note that we have, in fact, shown that the operator is conservative. Since our norm is related to the energy we have simply verified that the energy is constant (for the uncontrolled system). To complete the hypothesis of the theorem we must verify that the adjoint operator A^* is also dissipative. In fact we shall show more.

Lemma 2.2. The operator A is skew-adjoint.

Proof: Recall that the operator A^* is defined on its domain

$$D(A^*) = \{w / \text{there exists } w^* \in Z \text{ such that } \langle Ay, w \rangle - \langle y, w^* \rangle = 0 \\ \text{for all } y \in D(A)\}$$

by

$$A^*w = w^*.$$

We use this characterization to compute A^* .

Let $y = \text{col } (y_1, y_2, y_3, y_4(\cdot), y_5(\cdot)) \in D(A)$ and assume $w = \text{col } (w_1, w_2, w_3, w_4(\cdot), w_5(\cdot))$ and $w^* = \text{col } (w_1^*, w_2^*, w_3^*, w_4^*(\cdot), w_5^*(\cdot))$ satisfy

$$0 = \langle Ay, w \rangle - \langle y, w^* \rangle$$

Using the definition of A and the inner product \langle, \rangle we obtain the identity

$$\begin{aligned} 0 &= [y_4(0)(EIw_1) + y_4'(L)(EIw_2) - y_4(L)(EIw_3) \\ &\quad + EI \int_0^L y_5''(x)w_4(x)dv - EI \int_0^L y''(x)w_5(x)dx] \\ &\quad - [y_1(I_A w_1^*) + y_2(m_c w_2^*) + y_3(I_C w_3^*) \\ &\quad + EI \int_0^L y_4(x)w_4^*(x)dv + EI \int_0^L y_5(x)w_5^*(x)dv] . \end{aligned}$$

Collecting terms and applying the conditions that $y_1' = y_5'(0)$, $y_2 = y_5(L)$, $y_3 = y_5(L)$ and $y_5(0) = 0$, this equation becomes

$$\begin{aligned} 0 = & y_4(0) (EIw_1) + y_4(L) (EIw_2) + y_4(L) (-EIw_3) \\ & + y_5'(0) (-I_0Aw_1^*) + y_5(L) (-m_cw_2^*) + y_5(L)(-I_cw_3^*) \\ & + \int_0^L [y_5''(x) (EIw_4(x)) + y_5(x) (-\rho w_5^*(x))] dx \\ & + \int_0^L [y_4''(x) (-EIw_4(x)) + y_4(x) (-EIw_4^*(x))] dx, \end{aligned}$$

which must hold for all functions $y_4(x)$, $y_5(x)$ in the Sobolev space

$H^2(0,L)$ (see [1]). In particular, this equation holds for $y_4(x) = 0$ and

$y_5(x)$ satisfying $y_j(0) = y_j'(0) = y_j'(L) = y_j(L) = 0$, $i,j = 4,5$ which implies that

$$\int_0^L y_5''(x) (EIw_4(x)) + y_5(x) (-\rho w_5^*(x))] dx = 0$$

and

$$\int_0^L y_4''(x) (-EIw_5(x)) + y_4(x) (-EIw_4^*(x))] dx = 0.$$

The fundamental Lemma of the Calculus of Variations implies that

$w_4(\cdot)$ and $w_5(\cdot)$ belong to $H^2(0,L)$ and

$$w_5''(x) = w_4^*(x)$$

and

$$\frac{EI}{5} w_4''(x) = w_5^*(x).$$

Substituting for $w_4^*(x)$ and $w_5^*(x)$ in the integrals and integrating by parts, the equation

$$0 = \langle y, w \rangle - \langle y, w \rangle$$

becomes

$$\begin{aligned} 0 = & y_4(0) [EIw_1 - EIw_5'(0)] + y_5(0) [EIw_4'(0)] \\ & + y_4'(0) [EIw_5(0)] + y_5'(0) [-EIw_4'(0) - I_A w_1^*] \\ & + y_4(L) [-EIw_3 + EIw_5'(L)] + y_5(L) [-EIw_4'(L) - m_c w_2^*] \\ & + y_4'(L) [EIw_2 - EIw_5(L)] + y_5'(L) [EIw_4(L) - I_c w_3^*], \end{aligned}$$

which must hold for all values of $y_4(0)$, $y_4'(0)$, $y_4(L)$, $y_4'(L)$, $y_5(0)$, $y_5(L)$, $y_5'(L)$ and for $y_5(0) = 0$. Thus, it follows that

$$w_5'(0) = w_1, w_5(L) = w_2, w_5'(L) = w_3, w_5(0) = 0$$

and

$$w_1^* = \frac{-EI}{I_A} w_4(0), \quad w_2^* = -\frac{EI}{m_c} w_4'(L), \quad w_3^* = \frac{EI}{I_c} w_4(L).$$

Therefore, if $w \in D(A^*)$, then $w = \text{col}(w_1, w_2, w_3, w_4(\cdot), w_5(\cdot))$ is such that $w_4(x), w_5(x) \in H^2(0, L)$ with $w_1 = w_5'(0)$, $w_2 = w_5(L)$, $w_3 = w_5'(L)$, $0 = w_5(0)$, and

$$A^* w = \text{col} \left(\frac{-EI}{I_A} w_4(0), \frac{-EI}{m_c} w_4'(L), \frac{EI}{I_c} w_4(L), -w_5''(x), \frac{EI}{I_c} w_4''(x) \right) = -Aw.$$

Conversely, it is easy to show that if w is as above then $w \in D(A^*)$ and $A^* w = -Aw$. This completes the proof that $D(A^*) = D(A)$ and $A^* w = -Aw$. In particular, A is skew-adjoint.

Combining Lemmas 2.1 and 2.2 we have established the following.

Theorem 2.1: The operator defined by equations (2.8) and (2.10) generates a Co semigroup of contractions on the state-space $Y = \mathbb{R}^3 \times L_2 \times L_2$.

We have verified that the state-space model assembled from the formal system does indeed make sense. Before closing this section we note that the angular coordinate θ may be appropriate in the control problem. That is, we want to add a "zeroth" state, with equation $\dot{\theta}(t) =$

$\omega(t)$. To avoid duplicating much of the previous work, we shall do this by augmenting the state and "perturbing" the A operators.

Let $Z = R \times Y$ and consider the dynamical system

$$\dot{z}(t) = \hat{A} z(t) + \hat{B} f(t)$$

with

$$\begin{aligned} \hat{A}(\alpha, y) &= \begin{bmatrix} y_1 \\ -\frac{y_1}{Ay} \end{bmatrix} \\ \hat{B} &= \begin{bmatrix} 0 \\ -\frac{0}{B} \end{bmatrix} \end{aligned} \tag{2.12}$$

and

$$D(\hat{A}) = \{ (\alpha, y) \in R \times Y \mid \alpha \in R \text{ and } y \in n(A) \}.$$

The inner-product is extended in an obvious way

$$\langle (\alpha, y), (\beta, w) \rangle_Z = \frac{\alpha \cdot \beta}{2} + \langle y, w \rangle_Y.$$

It is clear that one can write \hat{A} as a sum

$$\hat{A} = A_0 + A_1$$

where

$$A_0(\alpha, y) = \begin{bmatrix} 0 \\ -\frac{0}{Ay} \end{bmatrix}$$

and

$$A_1(\alpha, y) = \begin{bmatrix} y_1 \\ -\frac{y_1}{0} \end{bmatrix}$$

It can be easily seen that A_0 generates a contraction semigroup on Z . The proof is exactly the same as that used to demonstrate that A generates a contraction semigroup on Y . Also it is clear that A_1 is a bounded linear operator. A standard result [7, p. 76] can be used to conclude that \hat{A} generates a C_0 semigroup on Z . It should be noted that \hat{A} is not conservative and hence $\|z(t)\|$ will not be constant in the unforced case. \hat{B} is obviously bounded.

III. THE CONTROL PROBLEM

In this section we formulate a general quadratic optimal control problem for distributed parameter systems and then review those results that are important for developing approximation and numerical schemes for computing feedback gains. Let Z , U and Λ be real Hilbert spaces. We use the symbol \langle, \rangle to denote the inner product in each space. The space Z is the state space, U is the space of control inputs and Λ is the space of outputs (observations). Furthermore, we assume that A with domain $D(A) \subseteq Z$ is the generator of a strongly continuous semigroup e^{At} on Z and $B: U \rightarrow Z$ and $v: Z \rightarrow \Lambda$ are continuous linear operators. We assume that $R: U \rightarrow U$ is continuous, linear, self-adjoint (i.e. $R = R^*$) and $\|R\| \geq m > 0$. Moreover, we define $Q = v^*v$.

The distributed parameter control system is governed by

$$\dot{z}(t) = Az(t) + Bu(t) \quad (3.1)$$

with output

$$y(t) = vz(t) \quad (3.2)$$

Given z_0 , the (mild) solution to (3.1) satisfying $z(0) = z_0$ is given by the variation of parameters formula

$$z(t) = e^{At}z_0 + \int_0^t e^{A(t-s)} B u(s) ds \quad (3.3)$$

We consider the problem of finding $u(\cdot) \in L_2(0, T; U)$ which minimizes

$$J(u) = \int_0^T (\langle Q z(s), z(s) \rangle + \langle R u(s), u(s) \rangle) ds, \quad (3.4)$$

where $z(t)$ is given by (3.3) for $0 \leq t \leq T$. This problem is the most direct extension of the standard finite-dimensional linear quadratic control problem.

It can be shown (see Gibson [3]) that the optimal control $u^*(t)$ is state feedback. In particular,

$$u^*(t) = -R^{-1} B^* \Pi(t) z(t), \quad (3.5)$$

where $\Pi(t) : Z \rightarrow Z$ is the solution to the operator Riccati integral equation

$$\Pi(t) = \int_t^T e^{A^*(n-t)} [Q - \Pi(n) B R^{-1} B^* \Pi(n)] e^{A(n-t)} dn. \quad (3.6)$$

It is important to note that in general (3.6) cannot be differentiated to produce a Riccati differential equation. This lack of "smoothness" is one reason that numerical methods for computing approximate (sub-optimal) gains have to be carefully designed.

Another feature that is apparent from (3.6) is that the adjoint operator A^* plays an important role in determination of $\Pi(t)$. For infinite-dimensional problems such as structural control, the operator A is a differential operator. It is not a continuous operator. The same

is true of A^* . Any approximation scheme used for computing sub-optimal gains must be based on a numerical algorithm that produces good approximations to A and A^* . This turns out to be a crucial point that is often overlooked in finite element and modal control approaches to these problems.

As we shall see below, computing numerical solutions to the Riccati equation (3.6) involves solving non-linear mixed integral and partial differential equations. This is a highly complex problem. There are other methods for computing the gain operator

$$K(t) = R^{-1} B^* \Pi(t)$$

directly. One such method, the Chandrasekhar algorithm, is ideally suited for these infinite-dimensional problems. In particular, it can be shown (see [8]) that the gain operator can be found by solving the coupled Chandrasekhar integral equations

$$K(t) = \int_t^T R^{-1} B^* \Sigma^*(\tau) L(\tau) d\tau \quad (3.7)$$

$$\Sigma(t) = ve^{A(T-t)} - \int_t^T \Sigma(\tau) B K(\tau) e^{A(\tau-t)} d\tau, \quad (3.8)$$

where $K(t): Z \rightarrow U$ and $\Sigma(t): Z \rightarrow A$ are bounded strongly continuous operators.

In many applications equations (3.7) - (3.8) are less difficult to solve numerically than equation (3.6). This is particularly true for

problems with a fixed finite number of sensors and actuators. Such problems occur in realistic formulations of structural control problems, and result in finite dimensional control and observation spaces, i.e. $U = \mathbb{R}^m$ and $\Lambda = \mathbb{R}^p$.

In order to illustrate the potential advantages of the Chandrasekhar algorithm, consider the control problem for the structure described in Sections 1 and 2. The state space is $Z = \mathbb{R}^4 \times \mathcal{L}_2(0,L) \times \mathcal{L}_2(0,L)$. The Riccati operator $\Pi(t): Z \rightarrow Z$ has the form

$$\Pi(t) = \begin{bmatrix} \Pi_{00}(t) & \Pi_{01}(t) \\ \Pi_{10}(t) & \Pi_{11}(t) \end{bmatrix}$$

where

$\Pi_{00}(t)$ is a 4×4 matrix and $\Pi_{ij}(t)$ have the representations

$$\Pi_{01}(t) \begin{bmatrix} \phi_1(\cdot) \\ \phi_2(\cdot) \end{bmatrix} = \int_0^L \begin{bmatrix} p_1(t,\tau) & p_2(t,\tau) \\ q_1(t,\tau) & q_2(t,\tau) \\ r_1(t,\tau) & r_2(t,\tau) \\ s_1(t,\tau) & s_2(t,\tau) \end{bmatrix} \begin{bmatrix} \phi_1(\tau) \\ \phi_2(\tau) \end{bmatrix} d\tau$$

$$\Pi_{10}(t) \begin{bmatrix} \eta_1 \\ \eta_2 \\ \eta_3 \\ \eta_4 \end{bmatrix} (x) = \begin{bmatrix} p_1(t,x) & q_1(t,x) & r_1(t,x) & s_1(t,x) \\ p_2(t,x) & q_2(t,x) & r_2(t,x) & s_2(t,x) \end{bmatrix} \begin{bmatrix} \eta_1 \\ \eta_2 \\ \eta_3 \\ \eta_4 \end{bmatrix}$$

and

$$\left\{ \begin{matrix} \Pi_{11}(t) \\ \left[\begin{matrix} \phi_1(.) \\ \phi_2(.) \end{matrix} \right] \end{matrix} \right\} (x) = \int_0^L \begin{bmatrix} \alpha_{11}(t,x,\tau) & \alpha_{12}(t,x,\tau) \\ \alpha_{21}(t,x,\tau) & \alpha_{22}(t,x,\tau) \end{bmatrix} \begin{bmatrix} z_1(\tau) \\ z_2(\tau) \end{bmatrix} d\tau$$

where $p_i, q_i, r_i, s_i, \alpha_{ij}$ $i, j = 1, 2$ are all L_2 functions. The Riccati equation (3.6) becomes a coupled integral-partial differential equation that must be solved to determine the 16 entries in $\Pi_{00}(t)$ and the 12 functions p_i, q_i, r_i, s_i and α_{ij} for $i, j = 1, 2$, $0 \leq t \leq T$, $0 \leq x \leq L$.

On the other hand since the operator $B = \text{col } (0, 1/I_A, 0, 0, 0, 0)$ has rank one the gain operator $K(t) = R^{-1}B^*(t)$ has rank one and $K(t)$ has the form

$$K(t)z(t) = \sum_{i=1}^4 \hat{K}_i(t)z_i(t) + \int_0^L \hat{K}_5(t,s)z_5(t,s)ds + \int_0^L \hat{K}_6(t,s)z_6(t,s)ds,$$

or equivalently,

$$\begin{aligned} K(t)z(t) = & K_1(t)\theta(t) + K_2(t)\omega(t) + K_3(t)\dot{\omega}(t) + K_4(t)\dot{\theta}(t) \\ & + \int_0^L K_5(t,s)u_{xx}(t,s)ds + \int_0^L K_6(t,s)[u_t(t,s)]ds. \end{aligned} \quad (3.9)$$

In order to determine the gain operator it is sufficient to determine the 6 functions K_i , $i = 1, 6$. The functions $K_5(t,s)$ and $K_6(t,s)$ are called the functional gains. These functions are linear combinations of

$q_i(t,s)$. Note that the functions a_{ij} , p_i , r_i , s_i , $i=1,2$ are not needed to define the gain operator.

If the observation operator v has finite rank, say $v: Z \rightarrow \mathbb{R}^p$, then $z(t)$ has the form

$$z(t)z = \sum_{i=1}^4 \vec{A}_i(t)z_i + \int_0^L \vec{A}_5(t,s)z_5(s)ds + \int_0^L \vec{A}_6(t,s)z_6(s)ds,$$

where the functions $\vec{A}_i(t)$ take values in \mathbb{R}^p $i = 1,2,3,4$ and $\vec{A}_i(t,s): \mathbb{R}^p$ for $i = 5,6$. In this case the Chandrasekhar equations involve coupled integral-partial differential equations to be solved for the 6 functions $K_i(t)$, $K_i(t,s)$, $0 \leq t \leq T$, $0 \leq s \leq L$ and the 6-p functions that are the entries in the \mathbb{R}^p valued vector functions $\vec{A}_i(t)$, $\vec{A}_i(t,s)$ for $0 \leq t \leq T$, $0 \leq s \leq L$. The main point to be made here is that the spatial dimension of the equations (3.7) - (3.8) is one, compared to equation (3.6) which has spatial dimension two. This reduction can be substantial when one attempts numerical solutions of the equations.

Perhaps the simplest way to see the real advantage of the Chandrasekhar algorithm is to apply it directly to the finite dimensional approximating system. An example of this type will be given in Section 4.

In order to obtain approximate solutions to the Riccati equation (3.6) or the Chandrasekhar equations (3.7) - (3.8) it is necessary to approximate the operators A , A^* , B , R , v and v^* . The most difficult aspect of this problem is the development of convergent approximation schemes for A and A^* . We shall need the following definitions.

Definition 1. An approximating sequence for the control problem defined by equations (3.3) - (3.4) is a sequence (A^N, B^N, v^N, R^N) such that A^N, B^N, R^N and $Q^N = [v^N]^* v^N$ are continuous linear operators satisfying $\|R^N\| \geq m \geq 0$, Q^N is non-negative definite, $B^N u \rightarrow Bu$ and $R^N u \rightarrow Ru$ for all $u \in U$, $Q^N z \rightarrow Qz$ for all $z \in Z$ and the operators A^N generate strongly continuous semigroups $e^{A^N t}$ satisfying

$$e^{A^N t} z \rightarrow e^{At} z \quad (3.11)$$

for all $z \in Z$, uniformly for $t \in [0, T]$

An approximating sequence is said to be a strong approximating sequence if the semigroup $e^{[A^N]^* t}$ generated by $[A^N]^*$ satisfies

$$e^{[A^N]^* t} w \rightarrow e^{A^* t} w \quad (3.12)$$

for all $w \in Z$ uniformly for $t \in [0, T]$

The construction of approximating sequences for the control problem (3.3) - (3.4) is a problem in numerical analysis and approximation theory. The basic idea is to approximate the (differential) operator by a finite-dimensional operator A^N (i.e. using finite elements, finite differences, modal truncation, etc.) and then showing that A^N converging to A implies (3.11) and (3.12). This is a nontrivial problem in functional analysis. In fact, the basic question (when does $A^N \rightarrow A$ imply (3.11) and (3.12)) is not yet fully understood. A partial answer

to the convergence question is provided by the now famous Trotter-Kato Theorem [11]. Although there are a number of extensions of this theorem (see Theorem 3.1 in [2]), we state a simple version that is sufficient for the problems considered here.

Theorem (Trotter-Kato). Let B be the generator of a strongly continuous semigroup e^{At} satisfying $\|e^{At}\| \leq Me^{\beta t}$. Assume that A^N is a sequence of operators generating strongly continuous semigroups $e^{A^N t}$ satisfying.

$$i) \|e^{A^N t}\| \leq Me^{\beta t}, \quad N=1,2,\dots$$

$$ii) A^N z \rightarrow Az \text{ for } z \in D, D \text{ dense in } Z$$

iii) there exists λ_0 with $\operatorname{Re}(\lambda_0) \geq \beta$ such that $(A - \lambda_0 I)D$ is dense in Z . Then $e^{A^N t} z \rightarrow e^{At} z$ for all $z \in Z$ and the convergence is uniform for $t \in [0, T]$.

In terms of numerical analysis, condition i) is the stability requirement and condition ii) is the consistency requirement. Thus convergence of the approximation scheme is dependent upon having a consistent and stable numerical scheme that also satisfies the technical condition iii). Any numerical scheme that does not satisfy conditions i) - iii) will not produce an approximating sequence for the control problem (3.3) - (3.4). Moreover, even if the approximating sequence is such that i) -

iii) are satisfied, there is no assurance that it will be a strong approximating sequence unless the operators $[A^N]^*$ and A^* also satisfy i) - iii).

The following convergence results are the basis for numerical algorithms for computing sub-optimal controls. The fundamental results are due to Gibson [3]. Powers [8] modified Gibson's results to apply to Chandrasekhar algorithms.

Theorem 3.1. Let (A^N, B^N, V^N, R^N) be an approximating sequence for the control problem (3.3) - (3.4). Let $\pi^N(t)$ be the solution to the Riccati equation

$$\begin{aligned} \dot{\pi}^N(t) = & - [A^N]^* \pi^N(t) - \pi^N(t) A^N - Q^N \\ & + \pi^N B^N [R^N]^{-1} [B^N]^* \pi^N(t), \quad 0 \leq t \leq T, \end{aligned} \quad (3.13)$$

with

$$\pi^N(T) = Q^N \quad (3.14)$$

i) If $\pi(t)$ is the solution to the Riccati integral equation (3.6), then for each $t \in [0, T]$, $z \in Z$, $\pi^N(t)z \xrightarrow{\text{weakly}} \pi(t)z$.

ii) If the approximating sequence is a strong approximating sequence, then $\pi^N(t)z \rightarrow \pi(t)z$.

iii) If, in addition, the control space U is finite dimensional and $v_z^N \rightarrow v_z$ for $z \in Z$, then for $0 \leq t \leq T$

$$\|K^N(t) - K(t)\| \rightarrow 0, \quad (3.15)$$

where

$K(t)$ is the gain operator defined by (3.7) - (3.8) and $K^N(t)$ is the solution to the Chandrasekhar equations

$$\frac{d}{dt} K^N(t) = -[R^N]^{-1} [B^N]^* [L^N(t)]^* L^N(t) \quad (3.16)$$

$$\frac{d}{dt} L^N(t) = -L^N(t) [A^N - B^N K^N(t)], \quad 0 \leq t \leq T \quad (3.17)$$

with

$$L^N(t) = v^N \text{ and } K^N(T) = 0. \quad (3.18)$$

A proof of this theorem will appear in a forthcoming paper. However, it is clear that from a practical point of view it is desirable to have uniform convergence of the gain operator (i.e. (3.15)) rather than weak convergence. Therefore, considerable effort should be devoted to constructing strong approximating sequences that have the additional property that $v^N \rightarrow v$. Such schemes are needed to ensure uniform con-

vergence of the approximating gain operators $K^N(t)$ (obtained from a finite dimensional Chandrasekhar algorithm) to the optimal gain operator $K(t)$.

IV. NUMERICAL PROCEDURES

We have seen that the dynamics of the physical system can be formulated as an abstract model. A control problem has been stated and its 'solution' given without introducing any approximations. In particular, for the linear quadratic problem of Section III one knows that the optimal control can be given in feedback form as:

$$\begin{aligned} M_A(t) = & K_1(t)\theta(t) + K_2(t)\omega(t) \\ & + K_3(t)\eta(t) + K_4(t)\xi(t) \\ & + \int_0^L K_5(t,s) u_{xx}(t,s) ds \\ & + \int_0^L K_6(t,s) U_t(t,s) ds \end{aligned} \tag{4.1}$$

The time-varying gains K_i , including the 'functional-gains' K_5 and K_6 , are computed from the 'solutions' of the Chandrasekhar Equations (3.7) and (3.8).

Calculation of these gains requires approximation of A and A^* as discussed in Section III. In this section we shall discuss some details for constructing these approximations. Since for our problem $A = -A^*$ one need only consider the task of approximating A . It should be noted that this simplification is not generally possible.

Recall that our state-space is $Z = \mathbb{R}^4 \times L_2 \times L_2$ and it is clear that this space is infinite-dimensional because of the L_2 "functions" in the Z_5 and Z_6 coordinates. One useful way to think about constructing the approximates of A^N is to imagine finite-dimensional subspaces $Z^N \subset Z$ in which the 'functional coordinates' are approximated as linear combinations of elementary functions. The choice here is to use splines [10].

Specifically, we take the interval $[0,1]$ and divide it into N equal subintervals with $(N+1)$ 'knots' at $x=0, 1/N, 2/N, \dots, 1$. Consider a set of interpolating splines with the property that $\phi_j^N(j/n) = \delta_{ij}$. The degree of these splines is not yet specified; in practice one might use piecewise linear (hat functions) or piecewise cubic elements.

Define $e_i^N \in Z$, $i = 0, 1, \dots, N$, by

$$e_i^N = (0, 0, 0, 0, \phi_i^N(x/L), 0)$$

and for $j = 1, 2, \dots, N$ let

$$e_{N+j}^N = (0, \int_0^1 \phi_j^N(x) dx, \phi_j^N(1), \int_0^1 \phi_j^N(x) dx, 0, \phi_j^N(x/L))$$

Finally let $e_{-2}^N = (1, 0, 0, 0, 0, 0)$ and $e_{-1}^N = (0, 1, 0, 0, 0, 0)$

The set $E^N = (e_{-2}^N, e_{-1}^N, \dots, e_{2N}^N) \subset Z$ is linearly independent and hence its span is a $(2N+3)$ dimensional subspace of Z (say $\text{span } E^N = Z^N$).

For ease of exposition let N_0 denote the set $N_0 = \{0, 1, 2, \dots, N\}$ and N_1 denote the set $N_1 = \{1, 2, 3, \dots, N\}$.

Note that the basis E^N has been arranged so that each e_i^N satisfies the boundary conditions needed to be in $D(A)$. The ease of this construction is a favorable result of our choice of state-space. That is, one could have eliminated the coordinates Z_3 and Z_4 (η and ξ) by identifying $\eta(t) = U_t(t, L)$ and $\xi(t) = U_{tx}(t, L)$. However, it would then be necessary to incorporate equations (1.27) and (1.28) as boundary conditions in the domain of A . This greatly complicates the task of constructing basis elements.

Continuing with the numerical aspects we shall display a matrix representation of A^N in terms of the basis E^N . Let $P^N : Z \rightarrow Z^N$ denote the orthogonal projection onto Z^N and (formally) write $A^N = P^N A P^N$. The j^{th} column in the matrix representation of A^N will be the image of the j^{th} basis element under A^N , represented in terms of the basis E^N . Since $A^N e = P^N A e$, the representation amounts to solving the usual normal equations (see [10]) for the best approximation of Ae in terms of the basis E^N .

Straight forward calculations reveal that

$$Ae_2^N = 0; \quad Ae_{-1}^N = \text{col} [1, 0, 0, 0, 0, 0],$$

$$A e_i^N = \begin{bmatrix} 0 \\ \frac{EI}{I_A} \phi_i(0) \\ \frac{EI}{m_c L} \phi_i'(1) \\ -\frac{EI}{I_c} \phi_i(1) \\ 0 \\ -\frac{EI}{\rho L^2} \phi_i'' \end{bmatrix}$$

$i \in N_0$

and

$$A e_{N+j}^N = \begin{bmatrix} 0 \\ 0 \\ 0 \\ 0 \\ \frac{1}{L^2} \phi_j'' \\ 0 \end{bmatrix}$$

$j \in N_1$

Note that we have suppressed notation indicating the dependence of the spline functions ϕ_i on the grid size parameter N . Also observe that one could approximate the second derivative operator (e.g. by differencing the first derivative) and hence allow A^N to operate on functions not smooth enough to be in $W^{2,2}$. This would be needed, for example, if the ϕ_i were linear splines.

The normal equations are of the form

$$G^N A^N = R^N \quad (4.2)$$

where G^N is the gram matrix with (i,j) element $\langle e_j^N, e_i^N \rangle$ and R^N is the matrix with (i,j) element $\langle e_i^N, A e_j^N \rangle$. From the form of the basis vectors it is readily seen that:

- i) e_{-2}^N and e_{-1}^N are each orthogonal to the remainder of E^N ;
- ii) $\langle e_{-2}^N, e_{-2}^N \rangle = 1/2$;
- iii) $\langle e_{-1}^N, e_{-1}^N \rangle = \frac{I_A}{2}$;
- iv) each e_i^N is orthogonal to each e_{N+j}^N ; $i \in N_0$, $j \in N_1$.

Hence G^N is block diagonal and, in particular

$$G^N = 1/2 \begin{bmatrix} G^N & \emptyset & \emptyset \\ \emptyset & G_1^N & \emptyset \\ \emptyset & \emptyset & G_2^N \end{bmatrix}.$$

Direct calculations reveal that

$$G_0^N = \begin{bmatrix} 1 & 0 \\ 0 & I_N \end{bmatrix} ,$$

$$G_1^N(i,j) = 2 \langle e_i^N, e_j^N \rangle$$

$$= EIL \int_0^L \phi_i(s) \phi_j(s) ds$$

$$i, j \in N_0,$$

and that

$$G_2^N(i,j) = 2 \langle e_{N+i}^N, e_{N+j}^N \rangle$$

$$= \rho L^3 \left[\frac{IA}{\rho L^3} \phi_i'(0) \phi_j'(0) \right.$$

$$+ \frac{Mc}{\rho} \phi_i(1) \phi_j(1) \quad (4.3)$$

$$+ \frac{Ic_j}{\rho L^3} \phi_i'(1) \phi_j'(1)$$

$$+ \left. \int_0^L \phi_i(s) \phi_j(s) ds \right]$$

$$i, j \in N_1$$

Note that the choice of B-splines, which are non-zero over only a 'small' portion of the unit-interval, means that the G^N matrices will be banded. The band-width increases with the degree of the splines.

Assembly of the R^N matrix proceeds in much the same way with $R^N(i,j) = \langle e_i^N, A e_j^N \rangle$. It is easily shown that

$$R^N = 1/2 \begin{bmatrix} R_{00}^N & R_{01}^N & \theta \\ \theta & \theta & R_1^N \\ \theta & R_2^N & \theta \end{bmatrix} \quad (4.4)$$

with

$$R_{00}^N = \begin{bmatrix} 0 & 1 \\ 0 & 0 \end{bmatrix}$$

$$R_{01}^N = \begin{bmatrix} EI \frac{\partial}{\partial x} \phi_j(0) \end{bmatrix} \quad (j \in N_0)$$

$$R_1^N(i,j) = \frac{EI}{L} [\phi_i(1) \phi_j'(1) - \phi_i(0) \phi_j'(0)$$

$$- \int_0^1 \phi_i'(s) \phi_j'(s) ds]$$

$$i \in N_0, j \in N_1$$

$$\text{and } R_2^N = [R_1^N]^T.$$

The block structure of G^N and R^N suggest a compatible partitioning of A^N in the normal equations. It is readily seen that

$$A^N = \begin{bmatrix} A_{00}^N & A_{01}^N & 0 \\ 0 & 0 & A_1^N \\ 0 & A_2^N & 0 \end{bmatrix}$$

The banded structure of G_1^N and G_2^N suggests that a Cholesky factorization may be an efficient way of generating the A_k^N matrices.

It is convenient to gather dimensional factors and write

$$G_1^N = (EI/L) \tilde{G}_1^N, G_2^N = (\rho L^3) \tilde{G}_2^N, \text{ and } R_1^N = (EI/L) \tilde{R}_1^N.$$

With this notation it follows that

$$A_{00}^N = \begin{bmatrix} 0 & 1 \\ 0 & 0 \end{bmatrix}$$

$$A_{01}^N = \frac{EI}{I_A} \begin{bmatrix} 0 & 0 & \cdot & \cdot & \cdot & 0 \\ \phi_0(0) & \phi_1(0) & \cdot & \cdot & \cdot & \phi_N(0) \end{bmatrix}$$

$$A_2^N = \frac{1}{L^2} \cdot [G_1^N]^{-1} \cdot [R_1^N]^T$$

$$A_2^N = \frac{-EI}{\rho L^4} \cdot [\tilde{G}_2^N]^{-1} \cdot [\tilde{R}_1^N]^T$$

Formally then for any N the system (2.1) is approximated by

$$\dot{x}^N(t) = A^N x^N(t) + B^N M_A(t)$$

where A^N is as above and B^N is found by projecting B onto Z^N .

The approximating solution is found from the x_i coordinates as

$$z^N(t) = \sum x_i(t) e_i^N$$

The vectors x^N and z^N are each of dimension $(2N+3)$. The calculations necessary to generate A^N are easily done on a computer once the ϕ_i^N functions are selected.

In order to illustrate these ideas a FORTRAN code was constructed. The code assembles the matrices required to evaluate the Chandrasekar equations (3.16) - (3.18). Since many of the matrices can be quite sparse, the code employs partitioned versions so that most of the zero entries are not involved. For illustrative purposes the basis functions are 'linear splines' [10] and all physical constants are taken to be unity. The output operator V in equation (3.2) "reads out" the first four state components (i.e. $\theta(t)$, $\omega(t)$, $\eta(t)$, $\xi(t)$); it "samples" $z_5(t) = u_{xx}(t, x)$ at $x = .2$ and $x = .4$; and, it "samples" $z_6(t) = (u_t(t, x) + x \omega(t))$ at $x = .3$ and $x = .7$. Thus, A has rank 8.

The differential equations (3.16) and (3.17) were numerically integrated backwards from the initial condition (3.18) for 10 time units. It was observed that the dependent variables κ^N and z^N were changing very slowly at that point and so these were taken to be "steady-state" values. Shown in Figure 3 are graphs of the kernel function $K_5(x)$ [cf equation 3.9] for $N = 4$ and $N = 8$. These results are somewhat preliminary. In practice one would continue to increase N at least until the observed differences were "small". Our research code had modest dimensions for the various arrays and so the maximum permissible N was rather limited. Note that with $N = 8$ the matrices κ^N and z^N in equations (3.16) and (3.17) are 1×19 and 8×19 , respectively.

V. THE TWO BEAM STRUCTURE

In this section we develop the equations of motion of the structure shown in Figure 4. It is assumed that members at the top and bottom are rigid bodies connected by two flexible beams of identical length L , the structure is allowed to pivot about a fixed pivot point, and that the motion is in a plane. The development of the model is achieved by the same method used to derive the equations of motion for the single beam with a tip mass. Since the derivation is very similar to the beam-tip mass problem, we shall simply summarize the equations below.

Let $u^1(t, x^1)$ and $u^2(t, x^2)$ denote the position of the mass element dm with respect to its undeflected position on beam 1 and beam 2, respectively. The angle $\psi(t)$ denotes the rotation of the structure about the pivot point and $\phi(t)$ is the angle of rotation of the top body measured from its undeflected position. Let θ denote the fixed angle that each beam makes with the bottom rigid body and note that (see the Free Body Diagram in Figure 5)

$$\sin \theta = h/L, \cos \theta = (A-C)/2L. \quad (5.1)$$

Using the Free Body Diagram in Figure 4 we obtain the following set of equations.

Bottom Rigid Body

$$-f_{x_1} \cos \theta + f_{y_1} \sin \theta + f_{x_4} \cos \theta - f_{y_4} \sin \theta + f_{p_x} = 0 \quad (5.2)$$

$$-f_{x_1} \sin \theta - f_{y_1} \cos \theta - f_{x_4} \sin \theta - f_{y_4} \cos \theta + f_{p_y} = 0 \quad (5.3)$$

$$\begin{aligned}
 M_{AC} + A/2 (f_{x1} - f_{x4}) \sin \theta + A/2 (f_{y1} - f_{y4}) \cos \theta + M_1 + M_4 \\
 = I_{ACM} \ddot{\psi}(t)
 \end{aligned}
 \quad (5.4)$$

Beam 1

$$f_{x1} + f_{x2} = -m_1 \frac{Ah}{B^2} \ddot{\psi}(t) \quad (5.5)$$

$$\begin{aligned}
 f_{y1} + f_{y2} = m_1 \left[\frac{R}{2} - \frac{A}{4} \left(\frac{A-C}{B} \right) \ddot{\psi}(t) - \frac{BK}{2} \ddot{\phi}(t) \right. \\
 \left. + u^1_{tt}(t, \frac{B}{2}) \right]
 \end{aligned}
 \quad (5.6)$$

$$\begin{aligned}
 M_2 - M_1 + Bf_{y2} = [I_{11} - \frac{A}{8} (A-C)m_1] \ddot{\psi}(t) - I_{i1} K \ddot{\phi}(t) \\
 + \int_0^L \rho x^1 u^1_{tt}(t, x^1) dx^1
 \end{aligned}
 \quad (5.7)$$

Beam 2

$$f_{x3} + f_{x4} = m_2 \frac{Ah}{B^2} \ddot{\psi}(t) \quad (5.8)$$

$$f_{y3} + f_{y4} = -m_2 \left[\left(\frac{B}{2} - \frac{A}{4} \left(\frac{A-C}{B} \right) \right) \ddot{\psi}(t) - \frac{BK}{2} \ddot{\phi}(t) + u^2_{tt}(t, \frac{B}{2}) \right] \quad (5.9)$$

$$\begin{aligned}
 M_3 - M_4 - Bf_{y3} = [I_{24} - \frac{A}{8} (A-C)m_2] \ddot{\psi}(t) - I_{24} K \ddot{\phi}(t) \\
 + \int_0^L \rho x^2 u^2_{tt}(t, x^2) dx^2
 \end{aligned}
 \quad (5.10)$$

Top Rigid Body (mass = m_c)

$$(f_{x_3} - f_{x_2}) \cos \theta + (f_{y_2} - f_{y_3}) \sin \theta = m_c h(K\ddot{\phi}(t) - \ddot{\psi}(t)) \quad (5.11)$$

$$(f_{x_2} + f_{x_3}) \sin \theta + (f_{y_2} + f_{y_3}) \cos \theta = 0 \quad (5.12)$$

$$\begin{aligned} & -(M_2 + M_3) + \frac{C}{2} (f_{x_2} - f_{x_3}) \sin \theta + \frac{C}{2} (f_{y_2} - f_{y_3}) \cos \theta \\ & = I_{CCM} [\ddot{\psi}(t) + \ddot{\phi}(t)] \end{aligned} \quad (5.13)$$

Observe that equations (5.4), (5.11) and (5.13) can be combined to produce the algebraic equation

$$\begin{aligned} & \left(\frac{\cos \theta}{m_c h} - \frac{CK}{2I_{CCM}} \right) (f_{y_3} - f_{y_2}) + \frac{(1+K)A \sin \theta}{2I_{ACM}} (f_{x_1} - f_{x_4}) \\ & = \left(\frac{\sin \theta}{m_c h} - \frac{CK}{2I_{CCM}} \right) (f_{y_3} - f_{y_2}) + \frac{(1+K)A \cos \theta}{2I_{ACM}} (f_{y_4} - f_{y_1}) \\ & \quad - \frac{(1+K)}{I_{ACM}} (M_1 + M_4) - \frac{K}{I_{CCM}} (M_2 + M_3) - \frac{(1+K)}{I_{ACM}} M_{AC} \end{aligned} \quad (5.14)$$

Let \bar{f}_y, \bar{f}_x denote the column vectors $\bar{f}_y = \text{col}(f_{y_1}, f_{y_2}, f_{y_3}, f_{y_4}) = (f_{y_1}, f_{y_2}, f_{y_3}, f_{y_4})^T$ and $\bar{f}_x = \text{col}(f_{x_1}, f_{x_2}, f_{x_3}, f_{x_4}) = (f_{x_1}, f_{x_2}, f_{x_3}, f_{x_4})^T$,

respectively. Combine the algebraic equations (5.5) (5.8) (5.12) and (5.14) into the one linear equation

$$\bar{M} \bar{f}_x = \bar{N} \bar{f}_y + R \quad , \quad (5.15)$$

where

$$\bar{M} = \begin{bmatrix} 1 & 1 & 0 & 0 \\ 0 & 0 & 1 & 1 \\ 0 & \sin \theta & \sin \theta & 0 \\ \frac{(1+K)A \sin \theta}{2I_{ACM}} & -\left(\frac{\cos \theta}{m_c h} + \frac{CK}{2I_{ACM}}\right) & \left(\frac{\cos \theta}{m_c h} + \frac{CK}{2I_{ACM}}\right) & -\frac{(1+K)A \sin \theta}{2I_{ACM}} \end{bmatrix} \quad (5.16)$$

$$\bar{N} = \begin{bmatrix} 0 & 0 & 0 & 0 \\ 0 & 0 & 0 & 0 \\ 0 & -\cos \theta & -\cos \theta & 0 \\ -\frac{(1+K)A \cos \theta}{2I_{ACM}} & -\left(\frac{\sin \theta}{m_c h} - \frac{CK}{2I_{ACM}}\right) & \left(\frac{\sin \theta}{m_c h} - \frac{CK}{2I_{ACM}}\right) & \frac{(1+K)A \cos \theta}{2I_{ACM}} \end{bmatrix} \quad (5.17)$$

and

$$\bar{R} = \begin{bmatrix} -\frac{m_1 Ah}{28} \ddot{\psi}(t) \\ \frac{m_2 Ah}{28} \ddot{\psi}(t) \\ 0 \\ -\frac{(1+K)}{I_{ACM}} (M_1 + M_4) - \frac{K}{I_{CCM}} (M_2 + M_3) \end{bmatrix} + \begin{bmatrix} 0 \\ 0 \\ 0 \\ -\frac{(1+K)M_{AC}}{I_{ACM}} \end{bmatrix} \quad (5.18)$$

We note that \bar{M}^{-1} exists and therefore \bar{F}_x can be determined as a function of \bar{F}_y and \bar{R} . In order to complete the model we need to provide equations for the elastic motion of the beams and the corresponding boundary conditions. These equations are;

$$u^1_{tt}(t, x^1) = \frac{E^1 I^1}{\rho I^1} u^1_{xxxx}(t, x^1) - x^3 [\ddot{\psi}(t) - K\dot{\phi}(t)] \quad (5.19)$$

$$u^2_{tt}(t, x^2) = \frac{E^2 I^2}{\rho I^2} u^2_{xxxx}(t, x^2) - x^2 [\ddot{\psi}(t) - K\dot{\phi}(t)] \quad (5.20)$$

with boundary conditions:

$$\begin{aligned} M_1 &= E^1 I^1 u^1_{xx}(t, 0) \\ \text{at } x^1 &= 0 \quad f_{y_1} = E^1 I^1 u^1_{xxx}(t, 0) \end{aligned} \quad (5.21)$$

$$u^1(t, 0) = 0$$

$$u^1_x(t, 0) = K\phi(t)$$

$$\text{at } x^1 = L \quad \begin{cases} M_2 = E^1 I^1 u_{xx}^1(t, L) \\ f_{y_2} = E^1 I^1 u_{xxx}^1(t, L) \\ u^1(t, L) = 0 \\ u_x^1(t, L) = (1-K)\phi(t) \end{cases} \quad (5.22)$$

$$\text{at } x^2 = 0 \quad \begin{cases} M_4 = E^2 I^2 u_{xx}^2(t, 0) \\ f_{y_4} = E^2 I^2 u_{xxx}^2(t, 0) \\ u^2(t, 0) = 0 \\ u_x^2(t, 0) = K\phi(t) \end{cases} \quad (5.23)$$

$$\text{at } x^2 = L \quad \begin{cases} M_3 = E^2 I^2 u_{xx}^2(t, L) \\ f_{y_3} = E^2 I^2 u_{xxx}^2(t, L) \\ u^2(t, L) = 0 \\ u_x^2(t, L) = (1+K)\phi(t) \end{cases} \quad (5.24)$$

Let $z(t)$ denote the vector

$$z(t) = (\psi(t), \dot{\psi}(t), u_{xx}^1(t, \cdot), \phi(t), \dot{\phi}(t), u_{xx}^2(t_1), u_t^2(t, \cdot))^T$$

and note that $z(t) \in [R^2 \times L^2(0, L, R^2)]^2$. Therefore, the state of the system is described by four functions $\phi, \dot{\phi}, \psi, \dot{\psi}$ and four L_2 valued function $u_{xx}^1, u_t^1, u_{xx}^2, u_t^2$.

Equations (5.19) (5.20), (5.4) and (5.11) can be written as the first order system

$$F\dot{z}(t) = Hz(t) + G M_{AC}(t) \quad (5.25)$$

where H is a boundary-differential operator on $Z = [R^2 \times L_2(0, L, R^2)] \times [R^2 \times L_2(0, L, R^2)]$, and F is a bounded non-singular operator. Let

$$A = (F^{-1}H) \quad B = F^{-1}G \quad (5.26)$$

and define

$$D(A) = \{z \in Z \mid z \text{ satisfies } H_1\} \quad (5.27)$$

where $z = (z_1, z_2, z_3(\cdot), z_4(\cdot), z_5, z_6, z_7(\cdot), z_8(\cdot))$

and H_1) i) $z_3(\cdot), z_4(\cdot), z_7(\cdot), z_8(\cdot)$ all belong to $W^{2,2}(0, L)$.

$$\begin{aligned} \text{ii) } z_4(0) &= 0, & z_4'(0) &= K z_6 \\ \text{iii) } z_4(L) &= 0, & z_8'(0) &= K z_6 \\ \text{iv) } z_8(0) &= 0, & z_8'(0) &= K z_6 \\ \text{v) } z_8(L) &= 0, & z_8'(L) &= (1+K) z_6. \end{aligned} \quad (5.28)$$

The specific form of F, H, G, A and B can easily be constructed from equations (5.4), (5.11), (5.19) and (5.20) by combining equation (5.15) with the equations (5.6), (5.7), (5.9), and (5.10). As in

the problem with the single beam, it is necessary to show that the operator A defined by (5.26) - (5.28) generates a dynamical system on Z . Numerical algorithms will be similar to the one in Section 4 above.

REFERENCES

1. Adams, R. A., Sobolev Spaces, Academic Press, New York, 1975.
2. Banks, H.J., Burns, J.A. and Cliff, E.M., Parameter estimation and identification for systems with delays, SIAM J. Control and Optimization, 19, 1981, 791-828.
3. Gibson, J.S., "The Riccati integral equations for optimal control problems on Hilbert spaces," SIAM J. Control and Optimization, 17, 1979, 533-565.
4. Hille, E., and Phillips, R.S. Functional Analysis and Semi-groups, AMS Colloq. Pub. Vol. 31, 1957.
5. Meirovitch, L. Elements of Vibration Analysis, McGraw-Hill, New York, 1975.
6. Miele, A., Flight Mechanics, Addison Wesley, Reading, MA, 1962. pp. 28-34.
7. Pazy, A. Semigroups of Linear Operators and Applications to Partial Differential Equations, Springer-Verlag, New York, 1983.
8. Powers, R.K., "Chandrasekhar equations for distributed parameter systems," Ph.D. Dissertation, VPI&SU, Blacksburg, VA, 1984.
9. Rudin, W. F., Principles of Mathematical Analysis, McGraw-Hill, New York, 1976.
10. Schultz, M.H., Spline Analysis, Prentice-Hall, Englewood Cliffs, NJ, 1973.
11. Trotter, H.F., "Approximations of Semi-groups of operators," Pacific J. Math. 8, 1958, 887-919.
12. Walker, J.A., Dynamical Systems and Evolution Equations, Plenum Press, New York, 1980.

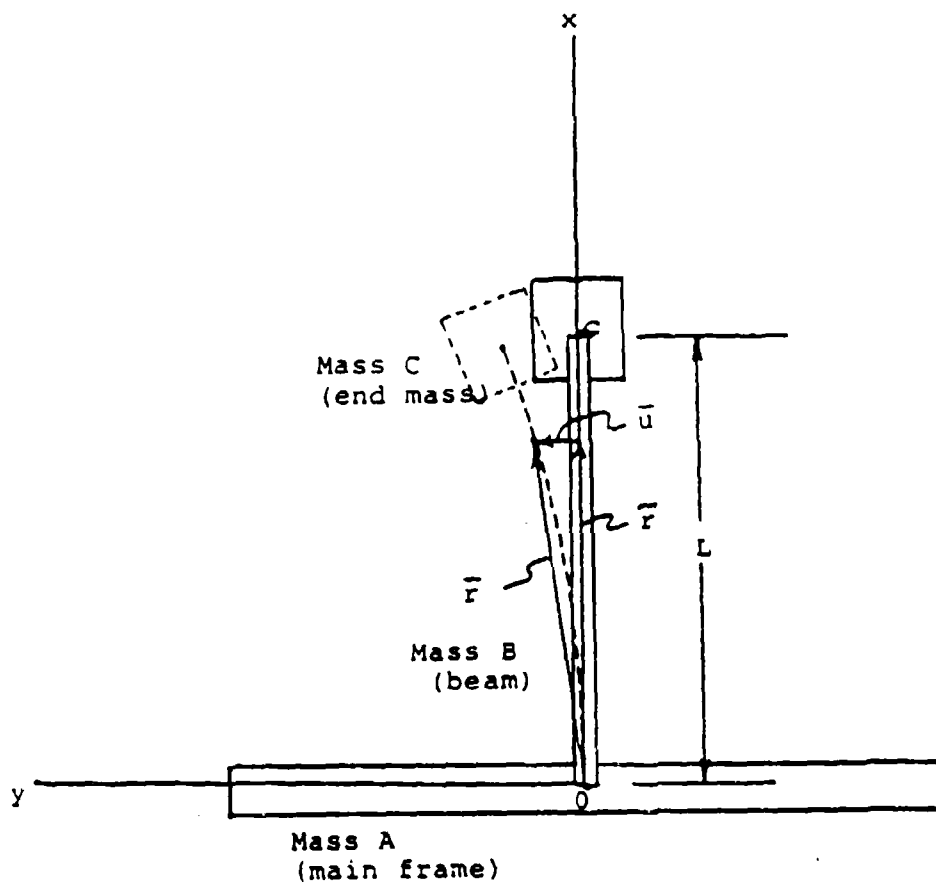


Figure 1 Flexible Structure.

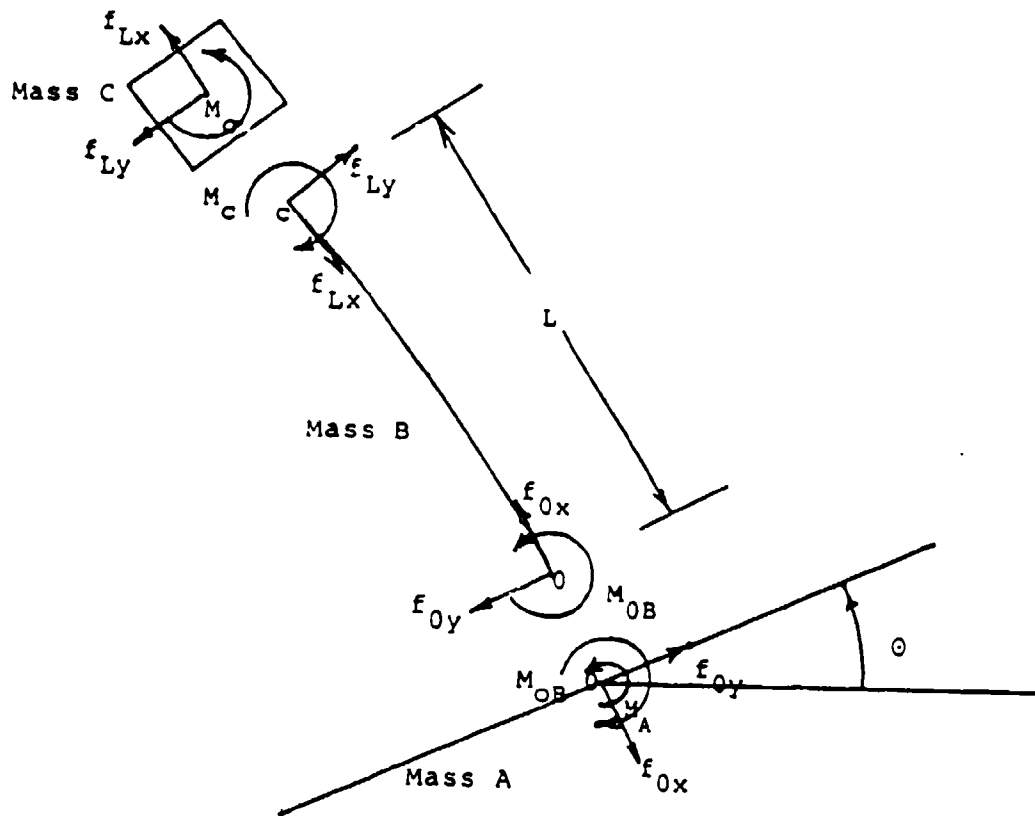


Figure 2 Free Body Diagram

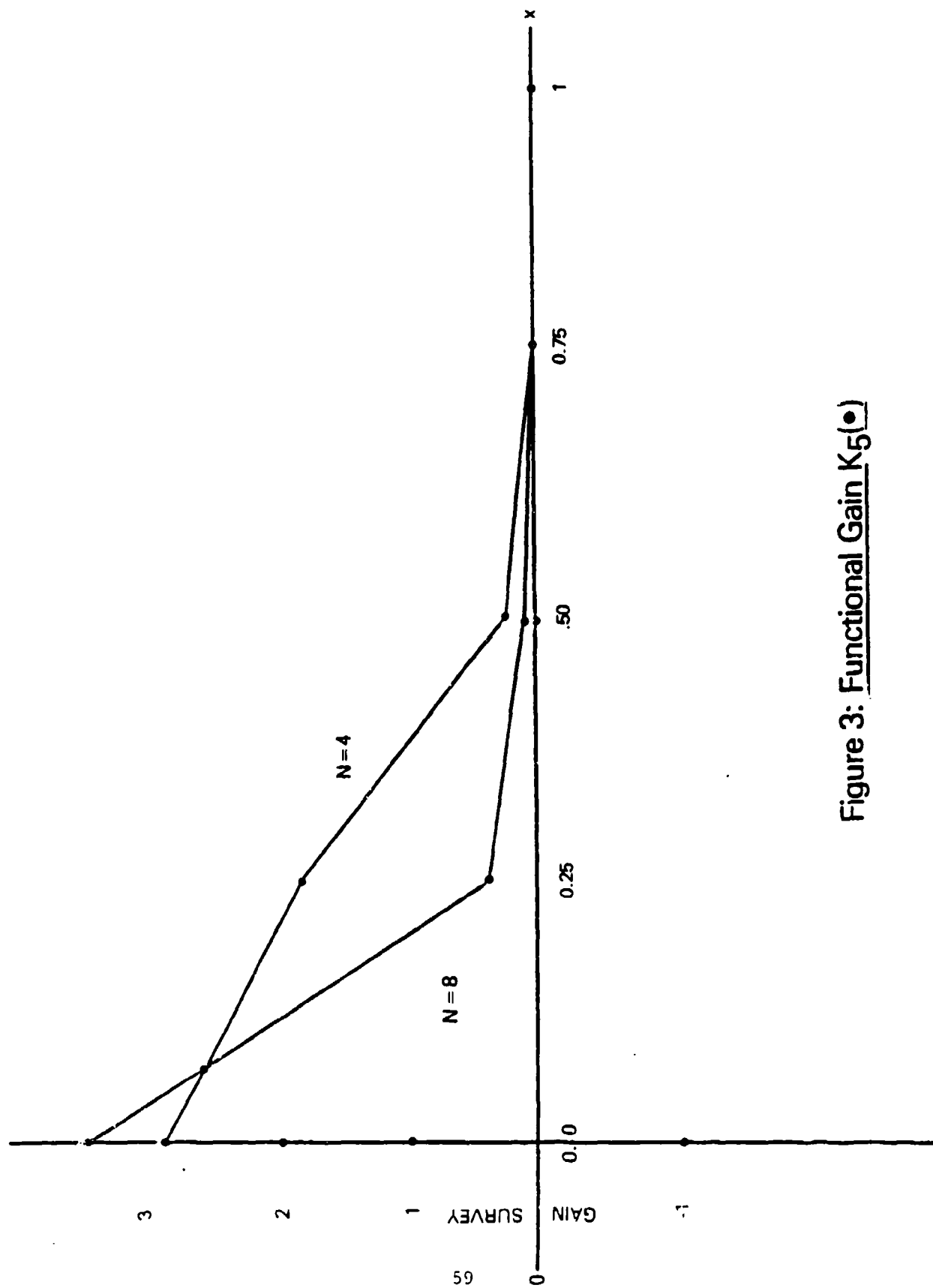


Figure 3: Functional Gain $K_5(\bullet)$

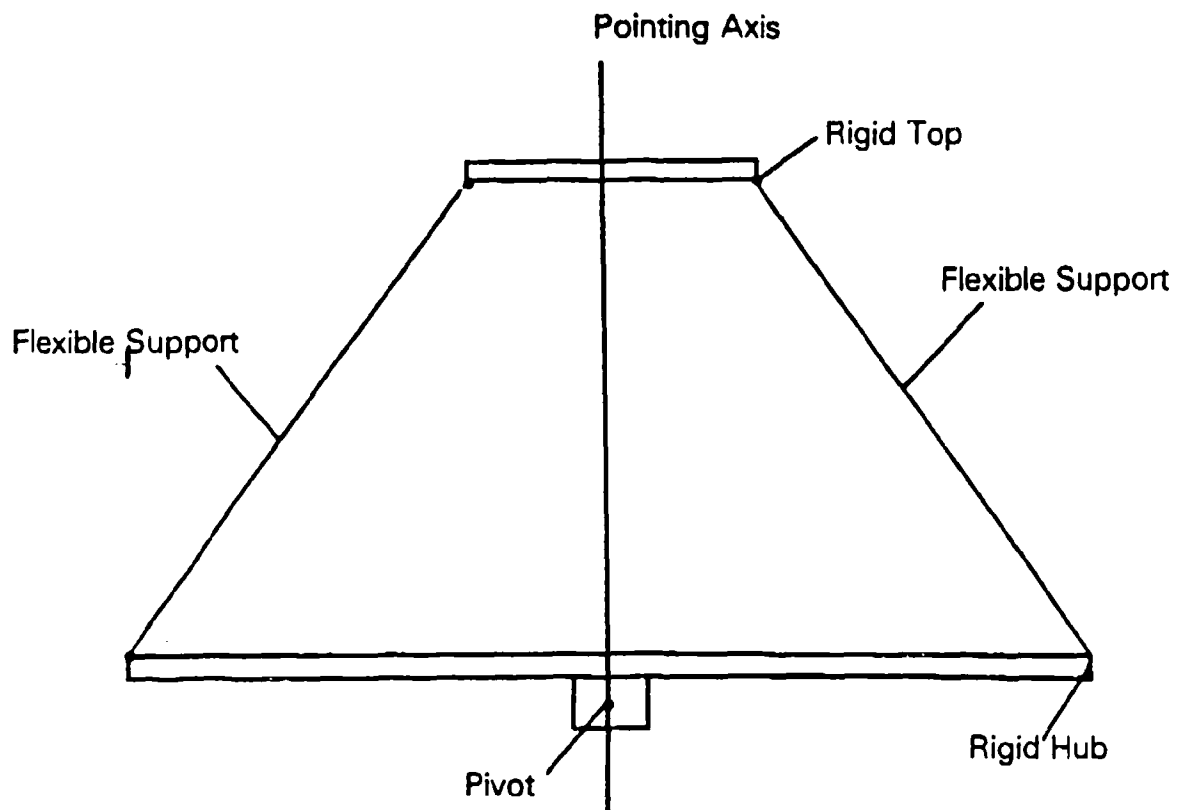


Figure 4: Prototype System

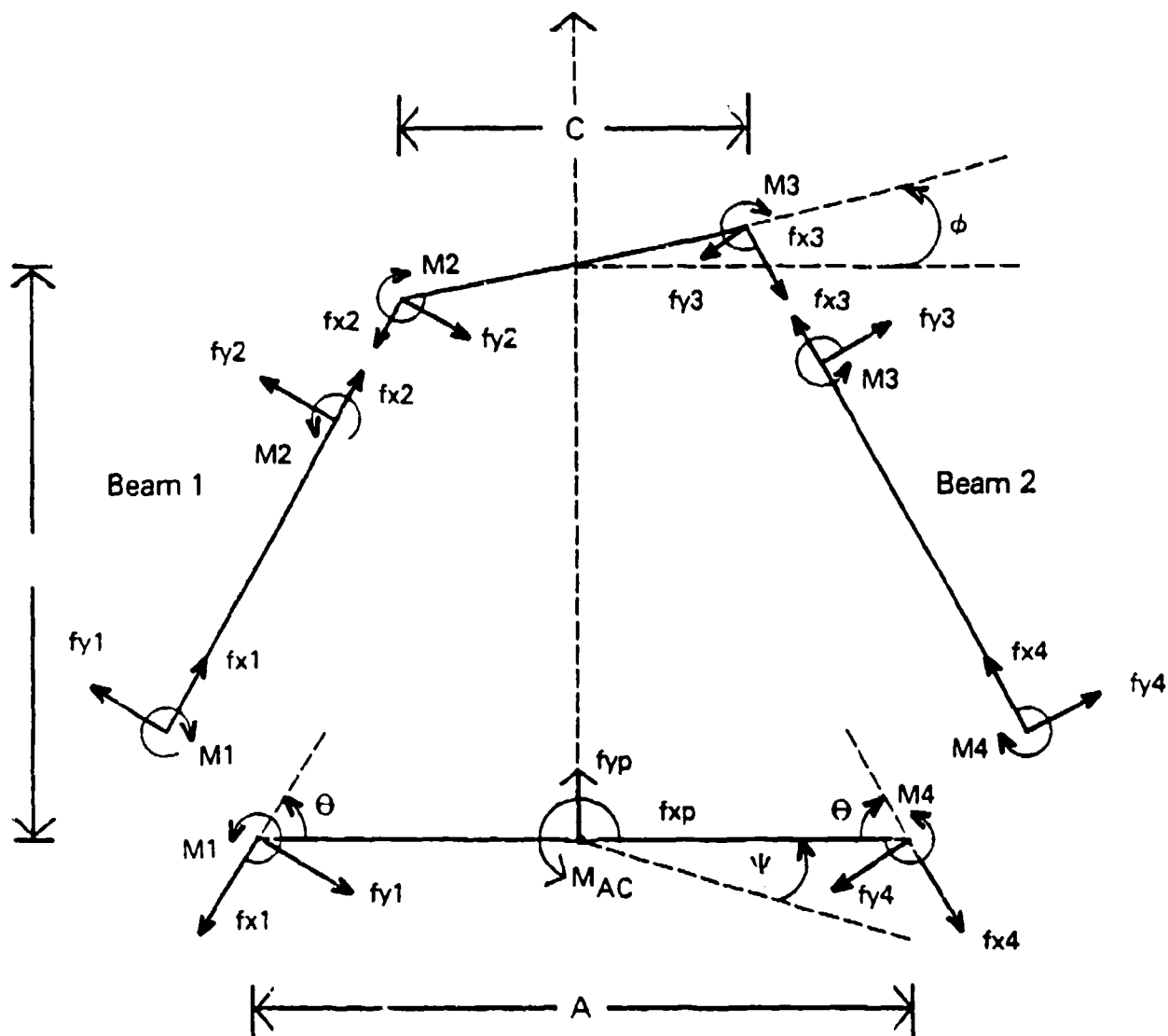


Figure 5: Free Body Diagram

PART II

EFFECTS OF TIME DELAY, ACTUATOR DYNAMICS
AND SYSTEM DAMPING ON THE FEEDBACK
CONTROL OF A FLEXIBLE CABLE

An Example of the Effect of Time Delay on Systems with Feedback which are Governed by Partial Differential Equations

I. Introduction

The purpose of this work is to offer some insight into some problems associated with the design of controllers for systems governed by partial differential equations. The method of analysis is based on the concept of transfer functions which relate the output or response of a system to the input. For simple structures, the displacement (velocity, or slope) can be related to the force applied by an exact transfer function. The accuracy of the transfer function is limited only by the accuracy of the mathematical model used to describe the structure. This open-loop transfer function can be used to construct the closed-loop transfer function for the case where the displacement (velocity, or slope) is fed back to the force. By examining the characteristic equation of the closed-loop transfer function the stability of the closed-loop system can be analyzed. This method will be applied to a flexible cable under tension.

It should be pointed out that although only a simple cable mass element will be considered here, the procedure can be used to examine more complex structures [1]. The advantage of the formulation used here is that it provides information in the form of root locus plots which are familiar to most and hence adds to the physical interpretation of the results. The inclusion of time delay in the problem does not change the method of analysis.

It is likely that in the near future almost all control systems will be digital in nature. Consequently the control command will always respond to the sensor inputs with a delay of at least one interval of sampling time associated with the controller. The contention to be demonstrated here is that regardless of how small this delay may be, it can cause some instability in systems with feedback. Because of its simplicity and familiarity, the analysis will be applied to the cable problem as indicated previously.

II. Flexible Cable Analysis

The vibrating cable is considered to be a continuous or distributed parameter system, that is, one governed by a partial differential equation. As shown in Figure 1a, $f(x,t)$, $\rho(x)$, and $T(x)$ are the distributed force, mass density, and tension in the cable, respectively, expressed as a function of position, x along the cable. For this analysis, negligible structural damping and no transverse stiffness is assumed.

The equation of motion describing the transverse motion of the cable can be obtained by examining a differential element of the cable. Figure 1b represents the free body diagram corresponding to a differential element of cable of length dx . Applying Newton's second law in the vertical direction, assuming small deflections, only vertical

motion and ignoring second-order terms in dx , we find that the governing partial differential equation of motion of the cable is given by [2]

$$\frac{\partial}{\partial x} \left[T(x) \frac{\partial y(x,t)}{\partial x} \right] + f(x,t) = \rho(x) \frac{\partial^2 y(x,t)}{\partial t^2}, \quad 0 \leq x \leq L \quad (2.1)$$

While Eq. (2.1) is the general equation of motion of the cable, it can be simplified by certain appropriate assumptions. In addition, any solution of Eq. (2.1) will depend on the particular boundary conditions of the cable configuration under consideration.

Fixed-free cable with a discrete mass at end

The configuration to be investigated is a cable of length L with constant mass per unit length, ρ , subjected to a constant tension T . This cable is fixed at one end, while the other end is free with a concentrated mass attached. A control force is acting vertically on the mass at the free end. Furthermore, there is no distributed force $f(x,t)$ acting along the cable, (see Figure 2a). For this particular problem Eq. (2.1) reduces to

$$\rho \frac{\partial^2 y(x,t)}{\partial t^2} = T \frac{\partial^2 y(x,t)}{\partial x^2}, \quad 0 \leq x \leq L \quad (2.2)$$

with the associated boundary condition at the fixed end $x = 0$,

$$y(0,t) = 0 \quad (2.3)$$

By writing Newton's second law for the free end, shown in Figure 2b, the boundary condition for the free end $x = L$ becomes,

$$f_L - T \left. \frac{\partial y(x,t)}{\partial x} \right|_{x=L} = m \left. \frac{\partial^2 y(x,t)}{\partial t^2} \right|_{x=L} \quad (2.4)$$

Eq. (2.2) can now be solved for the lateral deflection $y(x,t)$.

In the course of obtaining this solution we seek a relationship between the velocity at the end ($x=L$), (output) due to a force at the same end (input). This relationship is best expressed in terms of a transfer function which can be obtained by taking the Laplace transform of eq. (2.2) with respect to the time variable and evaluating the result at $x=L$. Since we are interested in the velocity, the result must be multiplied by the Laplace variable, s which is equivalent to the time derivative. The desired transfer function is given by

$$\frac{\dot{y}(L,s)}{f_L} = \frac{\sinh \sqrt{\rho/T} sL}{\sqrt{\rho T} \cosh \sqrt{\rho/T} sL + ms \sinh \sqrt{\rho/T} sL} \quad (2.5)$$

In order to simplify the problem further, we will set $\rho=T=1$. In addition it is convenient to allow the end mass to go to zero since this term only effects the uncontrolled frequencies and not the system stability. Equation (2.5) now reduces to

$$\frac{\dot{y}(L,s)}{f_L} = \frac{\sinh s}{\cosh s} = G(s) \quad (2.6)$$

Equation (2.6) is the open loop transfer function relating the velocity at the end to the force at the end of the fixed-free cable.

With eq. (2.6) as a starting point we can now examine the system characteristics for both open and closed loop control using root locus analysis.

III. Flexible Cable - Stability and Control

The system natural (open loop) frequencies can be obtained by setting the denominator of the transfer function equal to zero and solving for s , where $s = n + i\omega$. It is easily verified that the solution of $\cosh s = 0$ from Eq.(2.6) will yield imaginary values of s corresponding to the frequencies associated with a fixed-free cable. These are given by

$$n = 0, \quad \omega_k = \frac{2k-1}{2} \pi \quad k = \pm 1, \pm 2, \dots \quad (2.7)$$

where k is an integer which serves to identify a frequency.

Feedback Control

The system has open loop input, f_L and output \dot{y} related through $G(s)$. We now close the loop by feeding back velocity with a gain K , see Figure 3.

The closed loop transfer function can be shown to be

$$G(s)_{CL} = [1 + KG(s)]^{-1} G(s) \quad (3.1)$$

The closed-loop system dynamics can be determined from the closed-loop characteristic equation

$$1 + K G(s) = 0 \quad (3.2)$$

Now all the classical tools for control design can be used [3].

For velocity feedback at the cable end, the open-loop transfer function was shown to be

$$G(s) = \frac{\sinh s}{\cosh s} \quad (2.6)$$

Using Eq. (3.2) the associated closed-loop characteristic equation becomes

$$\cosh s + K \sinh s = 0 \quad (3.3)$$

If we let $s = n + i\omega$ we can obtain an analytic solution for the feedback by velocity. The results are given by

$$\tanh n = -K \quad ; \quad \omega = \frac{m\pi}{2} \quad (m \text{ odd}) \quad (3.4)$$

$$\tanh n = -\frac{1}{K} \quad ; \quad \omega = \frac{m\pi}{2} \quad (m \text{ even})$$

The root locus plot is shown in Figure 4.

It is seen from the root locus that all the modes are controlled by feeding back the velocity at the end of the cable to a force at the end. Furthermore no special filter is needed to process the sensor signal. For this particular case all modes are affected the same for a given gain. For gains less than one, the frequencies of vibration are the same as the open-loop frequencies but the motion is damped out. For gains greater than one the frequencies jump to those of a fixed-fixed

cable and the motion is also damped. At a gain of one, $n = -\infty$ and it can be shown that the system comes to rest in a finite time [4].

Although this simple problem can be solved analytically, the more general problem to follow would become analytically tedious. Consequently, a numerical method is used. Most computer routines that generate root-loci need to be supplied with polynomial functions or factors [5]. In this work the solution of a transcendental equation is required. One method of solution, for the generation of the root loci, is the use of a computer code which includes an IMSL routine called ZSCNT which solves for the roots of a set of non-linear simultaneous equations [6]. The complex characteristic equation, Eq. (3.3) is one of these sets when separated into real and imaginary equations. The procedure is to apply repeatedly the ZSCNT routine starting with the open-loop pole position with zero gain. Then, incrementing the gain, solve for the first closed-loop pole position. This pole is then used as the start point for solving for the pole at the next higher gain value and so on. This method is found to be highly reliable for calculating root-loci, although occasionally sensitive to abrupt changes in locus direction. A program listing with an example input and output file is given at the end of this report.

Feedback Control with Time Delay

Time delay is now introduced into the system such that the feedback of velocity is described by the diagram in Figure 5. As we have deter-

mined previously, the open-loop velocity force transfer function for the fixed-free cable is

$$G(s) = \frac{\sinh s}{\cosh s} \quad (2.6)$$

Adding the time delay of $e^{-s\tau}$ to the feedback loop yields a closed loop transfer function of the form

$$G(s)_{CL} = \frac{G(s)}{1 + K e^{-s\tau} G(s)} \quad (3.5)$$

which results in the characteristic equation

$$\cosh s + K e^{-s\tau} \sinh s = 0 \quad (3.6)$$

or

$$\cosh s + K (\cosh s\tau - \sinh s\tau) \sinh s = 0 \quad (3.7)$$

By letting $s = n + i\omega$ and incrementing the gain, K for a fixed time delay, τ , the root locus for the cable with delayed feedback of velocity can be obtained. The root locus for time delays of 0.1, 0.5, and 0.9 are shown in Figures 6, 7, and 8, respectively. These diagrams show clearly that unlike the no delay case that for any delay there are associated unstable roots. A relationship between the delay time and the unstable roots can be determined as follows:

Starting with the characteristic equation for the cable with delay eq.(3.7) we can note that it has the form of

$$F(s, k, \tau) = 0 \quad (3.8)$$

Letting $s = n + i\omega$ and expanding yields a real equation and an imaginary equation of the forms

$$R(n, \omega, K, \tau) = 0 \quad (3.9)$$

and

$$I(n, \omega, K, \tau) = 0 \quad (3.10)$$

If we select a particular value of τ we can suppress its dependence in eqs. (3.9) and (3.10). Further we can note that the real and imaginary parts of the solution along any branch of the root locus are functions of the gain K . Hence eqs. (3.9) and (3.10) take the form

$$R(n(K), \omega(K), K) = 0 \quad (3.11)$$

and

$$I(n(K), \omega(K), K) = 0 \quad (3.12)$$

By using the derivative chain rule we find

$$\frac{\partial R}{\partial n} \frac{dn}{dK} + \frac{\partial R}{\partial \omega} \frac{d\omega}{dK} + \frac{\partial R}{\partial K} = 0 \quad (3.13)$$

and

$$\frac{\partial I}{\partial n} \frac{dn}{dK} + \frac{\partial I}{\partial \omega} \frac{d\omega}{dK} + \frac{\partial I}{\partial K} = 0 \quad (3.14)$$

We are interested in solving for the quantity $\frac{dn}{dK}$ at the point where $K = n = 0$. Evaluated at these conditions $\frac{dn}{dK}$ describes how the real part of the solution departs from the zero gain roots on the imaginary axis. A positive value would yield instability for a small gain.

Solving for $\frac{dn}{dK}$ or n' yields

$$n' = \frac{R_{\omega} I_K - R_K I_{\omega}}{R_n I_{\omega} - R_{\omega} I_n} \quad (3.15)$$

where the subscripts indicate the partial derivatives in (3.13) and (3.14).

Applying eq. (3.15) to the characteristic equation for our system (3.7) yields the simple result

$$n' = -\cos \omega \tau \quad (3.16)$$

Hence instability occurs when $n' > 0$ or

$$\cos \omega \tau < 0 \quad (3.17)$$

Therefore, the system would be unstable if

$$\frac{\pi}{2} < \omega \tau < \frac{3\pi}{2} \quad (3.18)$$

$$\frac{5\pi}{2} < \omega \tau < \frac{7\pi}{2}$$

etc.

If we deal only with the first cycle and substitute the value for ω given by eq. (2.7), eq. (3.18) can be rewritten in the form

$$\frac{1}{2} \left(\frac{1}{\tau} + 1 \right) < k < \frac{1}{2} \left(\frac{3}{\tau} + 1 \right) \quad (3.19)$$

From eq. (3.19) it can be observed that for a value of delay there will be a value of k (k_k) for which the system is unstable. To demonstrate the validity of this result we can return to the numerical results we displayed previously. For the three time delays of interest we have

$\tau = 0.1$	$5.5 < k < 15.5$
$\tau = 0.5$	$1.5 < k < 3.5$
$\tau = 0.9$	$1.05 < k < 2.16$

Since k must be an integer, these values describe particular frequencies which would be driven unstable for small gain. Also from Figures 6, 7, and 8 it can be seen that the cycles are repeated as indicated by eq. (3.18).

IV. Feedback Control with First Order Actuator

The previous investigation showed the effect of a control system which included pure delay on the stability of a fixed-free cable. The purpose of this section is to show the effect a first order actuator might have on the cable stability both with and without a pure delay.

First Order Actuator without delay

We will initiate the study by placing a first order actuator in the system as described by Figure 9. Here the time constant associated with the first order system is designated by τ . From the figure, the closed loop transfer function can be shown to be

$$G(s)_{CL} = \frac{G(s)}{1 + \frac{K}{\tau s + 1} G(s)} \quad (4.1)$$

where $G(s)$ is given by eq. (2.6). The resulting characteristic equation is given by

$$\cosh s + s \tau \cosh s + K \sinh s = 0 \quad (4.2)$$

By letting $s = n + i\omega$, and incrementing the gain K for a fixed value of τ , the root locus for the cable with velocity feedback through a first order actuator can be obtained using procedures described previously.

The resulting root locus for values of τ of 0.1 and 0.5 are shown in Figures 10 and 11 respectively. These diagrams show that the first order actuator by itself does not lead to any unstable roots for any gain. However the strong stability characteristics displayed by direct feedback as shown in Figure 4 are severely reduced, especially at the higher frequencies. This result is easily explained by noting that the first order actuator has a finite bandwidth and hence does not respond very well to the frequencies outside of this bandwidth. Typically the bandwidth of a first order system is characterized by $\omega_B = 1/\tau$. For our two cases, $\omega_B = 10$ and 2 for Figures 10 and 11 respectively. Consequently, frequencies above these values are not affected as much as those below. However, as indicated previously, the control over those frequencies below the respective bandwidth frequencies is considerably reduced over the case where the actuator dynamics is ignored. One would expect that to control even low frequencies, an actuator with a large bandwidth is required.

First Order Actuator with Delay

We can now include a pure delay in conjunction with a first order actuator. This situation might occur if a digital control system is

used to drive the actuator. The block diagram displaying this type of set up is shown in Figure 12. From this diagram we can develop the closed loop transfer function which is given by

$$G(s)_{CL} = \frac{G(s)}{1 + \frac{K e^{-s\tau}}{\tau s - 1} G(s)} \quad (4.3)$$

which leads to the characteristic equation

$$\cosh s + s\tau \cosh s + K (\cosh s\tau - \sinh s\tau) \sinh s = 0 \quad (4.4)$$

Proceeding in the same manner as before, the root locus for a cable with velocity feedback thru a first order actuator with delay can be determined.

The root loci for the cases where $\tau = 0.1$ and 0.5 are shown in Figures 13 and 14 respectively. It can be observed that in both cases, the pattern of stable and unstable roots is the same as that which occurred with pure delay. The first frequency at which instability occurs however is slightly lower for the case of a first order actuator with delay than that with pure delay.

V. Feedback Control with System Damping

The various types of damping that could be considered are structural, viscous, and Coulomb [8]. The viscous damping model is

chosen here, as this model is the most easily understood and most widely used.

The Fixed-Free cable model for a constant tension cable with viscous damping is given by eq. (2.1) or

$$cy_t(x,t) + \rho y_{tt}(x,t) = Ty_{xx}(x,t) \quad (5.1)$$

where the viscous damping is

$$cy_t(x,t) = -f(x,t) \quad (2.2)$$

The boundary condition at the fixed end, $x=0$ is

$$y(0,t) = 0 \quad (2.3)$$

and at the free end, $x=L$ is

$$f_L - Ty_x(x,t) \Big|_{x=L} = my_{tt}(x,t) \quad (2.4)$$

The transfer function of this model can be obtained by taking the Laplace transform of eq. (5.1) with respect to the time variable and evaluating the result at $x=L$. Again we are interested in the velocity - force transfer function. For the case where the end mass is zero, this transfer function now has the form

$$G(s) = \frac{\dot{Y}(L,s)}{f_L} = \frac{s \sinh \sqrt{s^2 + cs}}{\sqrt{s^2 + cs} \cosh \sqrt{s^2 + cs}} \quad (5.3)$$

The system diagram for the damped system is illustrated in Figure 3 with $G(s)$ now given by eq. (5.3).

The closed-loop characteristic equation is given by

$$\sqrt{s^2 + cs} \cosh \sqrt{s^2 + cs} + K s \sinh \sqrt{s^2 + cs} \quad (5.4)$$

By letting $s = n+i\omega$ for fixed damping coefficient, c and incrementing the gain, K , the root locus can be obtained as before.

The addition of damping to the closed-loop system merely shifts the root loci from poles with zero real parts to poles that have negative real parts. The diagram will look like Figure 4 with starting and ending points shifted into the left half plane and again no unstable roots.

Feedback Control with System Damping and Delay

A more interesting result is obtained by adding time delay to a system with damping. The closed-loop characteristic equation of this case is given by

$$\sqrt{s^2 + cs} \cosh \sqrt{s^2 + cs} + Ks (\cosh s\tau - \sinh s\tau) \sinh \sqrt{s^2 + cs} \quad (5.5)$$

By letting $s = n + i\omega$ and incrementing the gain, K for a fixed time delay, and a fixed damping coefficient, c , the root locus for the cable with damping and delayed feedback of velocity can be obtained. The root locus for time delay of 0.1 and damping coefficients of 0.1 and 1.0 are shown in Figures 15 and 16 respectively. These diagrams are comparable to the diagram in Figure 6, but shifted to the left by an amount proportional to the damping coefficient. This observation leads to the conclusion that given sufficient damping the system is stable for small values of gains even with time delay.

VI. Closure

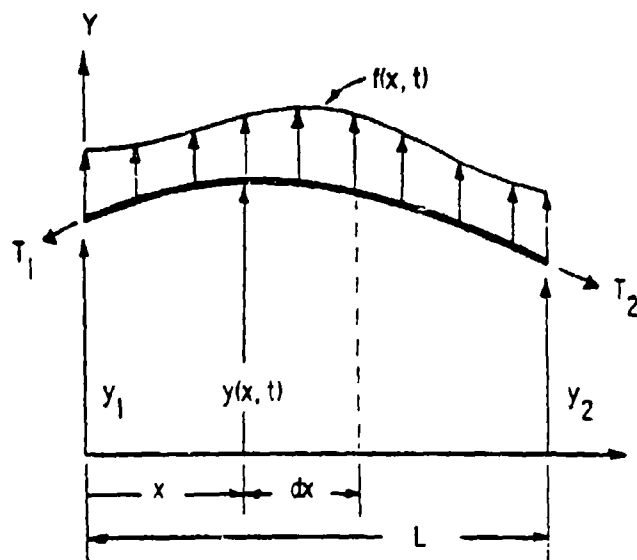
The cable problem discussed in this report can be made extremely stable by feeding back velocity at the end of the cable to a co-located force at the end of the cable. However it was shown that if any delay at all is used in implementing this feedback control, the system becomes unstable. This result was determined analytically with no restrictive assumptions other than those made for the original governing equation. The results were confirmed for selected numerical calculations.

In addition the results of a first order actuator and a first order actuator with delay were presented indicating that any delay leads to instability. Without delay the first order actuator does not lead to instability but is considerably less effective in stabilizing the cable than if no actuator dynamics were present. Further, the effects at higher frequencies are limited due to the bandwidth of the actuator.

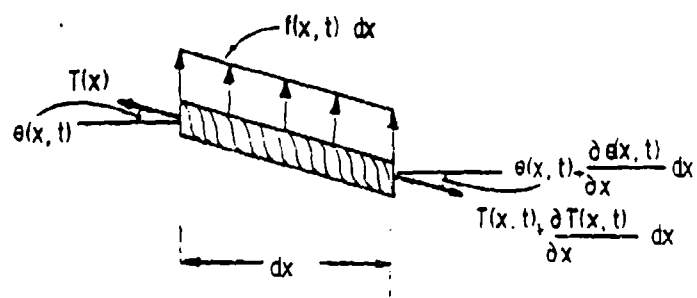
The addition of damping shifts the whole root locus to the left and allows a system with pure delay to remain stable for a small amount of gain.

REFERENCES

1. Lutze, F. H. and Goff, R. M. A. "Application of Classical Techniques to Control of Continuous Systems," Third VPI&SU Symposium, Blacksburg, VA, June 1981.
2. Meirovitch, L. Elements of Vibrations Analysis, McGraw-Hill, Inc., New York,, 1975, pp. 79-80.
3. D'Azzo, J. J. and Houpis, C. H. Linear Control System Analysis and Design, McGraw-Hill, Inc., New York, 1975.
4. Parks, P. C. "On How to Shake a Piece of String to a Standstill," Recent Mathematical Developments in Control, Academic Press, 1973, 1973, pp. 267-287.
5. Melsa, J. L. and Jones, S. K., Computer Programs for Computational Assistance in the Study of Linear Control Theory, Second Edition, McGraw-Hill, New York, 1973, pp. 114-120.
6. International Mathematical and Statistical Libraries, IMSL, Edition 8, IMSL, Inc., Houston, Texas, July 1980.
7. Gevarter, W. B. "Basic Relations for Control of Flexible Vehicles," AIAA Journal, Vol. 8, No. 4, Apr. 1970, pp. 666-672.
8. Hurty, W. C. and Rubinstein, M.F. Dynamics of Structures, Prentice-Hall, Inc., N.J., 1964, p. 257.

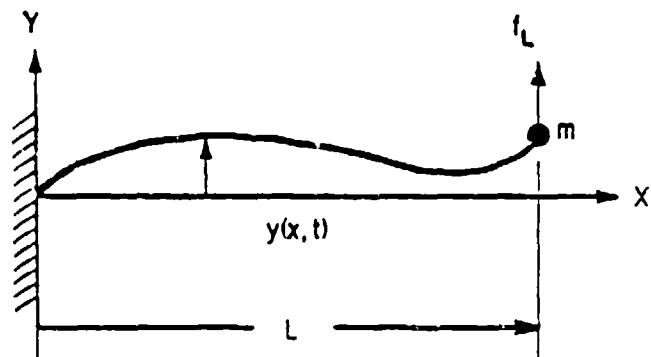


(a)

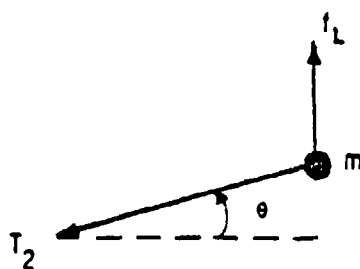


(b)

Figure 1 Cable Element



(a)



(b)

Figure 2 Fixed-Free Cable (discrete mass at end)

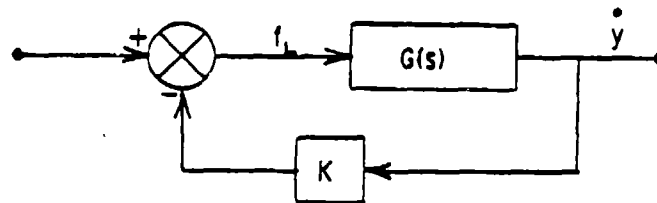
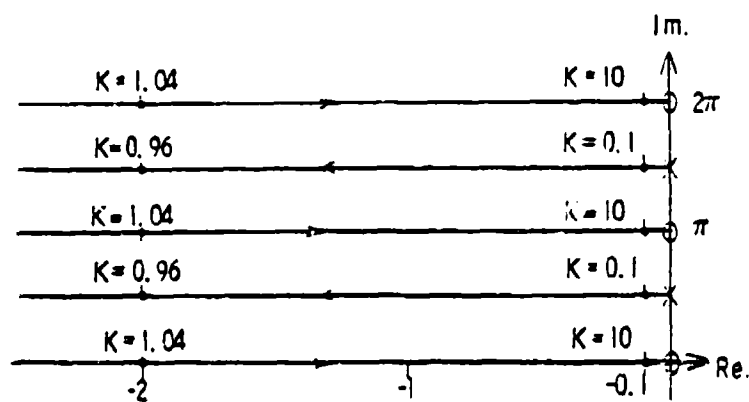


Figure 3 Feedback System



Characteristic Equation

$$\cosh s + K \sinh s = 0$$

Figure 4 End-End Velocity Feedback Root Locus
(Fixed-Free Cable)

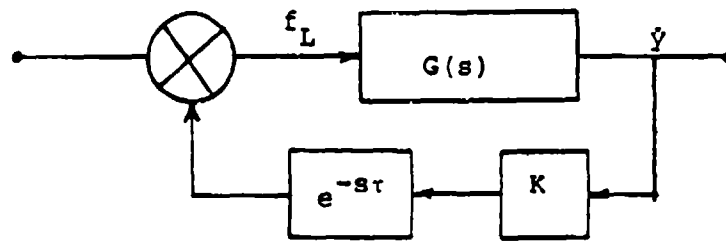
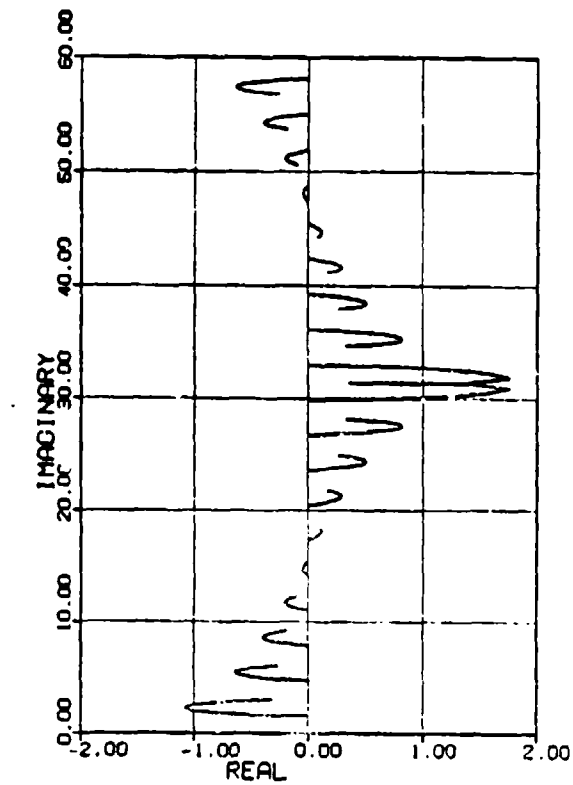


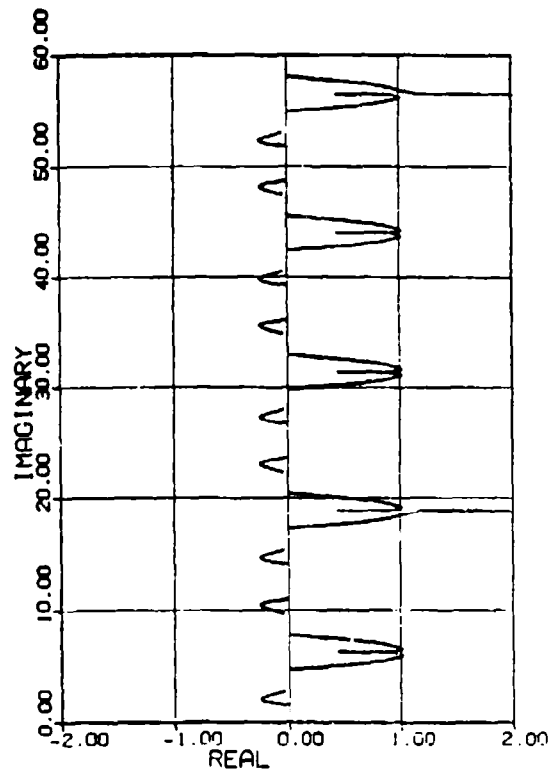
Figure 5 Feedback System With Delay



FIXED-FREE CABLE FEEDING BACK VELOCITY

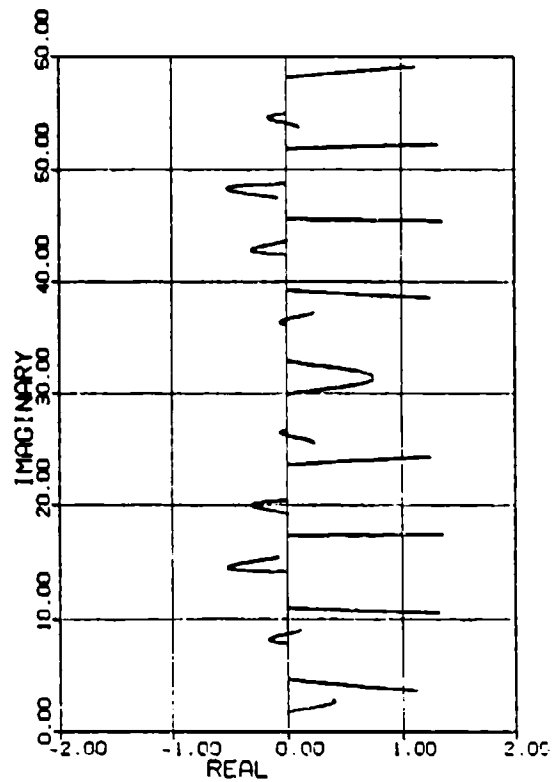
TO FORCE AT END. DELAY = 0.1

Figure 6



FIXED-FREE CABLE FEEDING BACK VELOCITY
TO FORCE AT END. DELAY = 0.5

Figure 7



FIXED-FREE CABLE FEEDING BACK VELOCITY
TO FORCE AT END. DELAY = 0.9

Figure 8

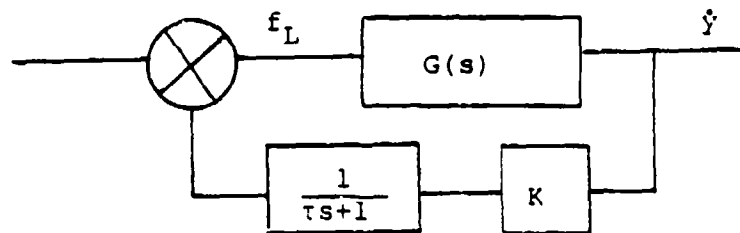
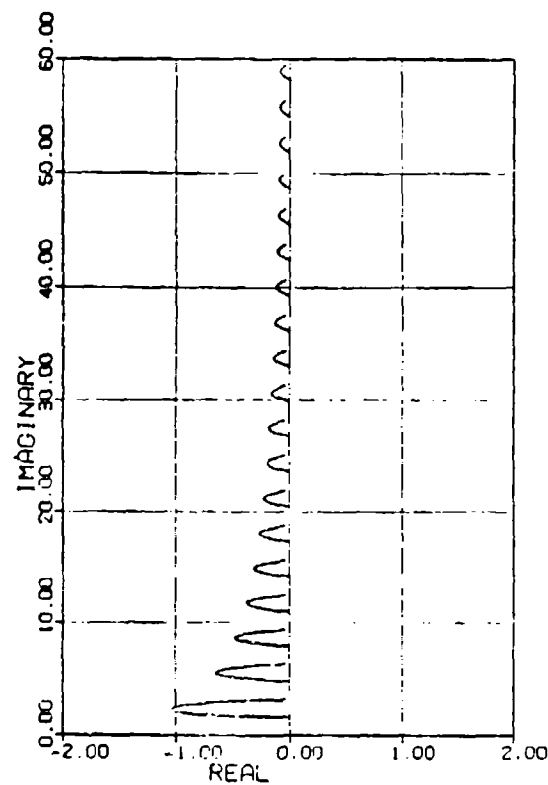
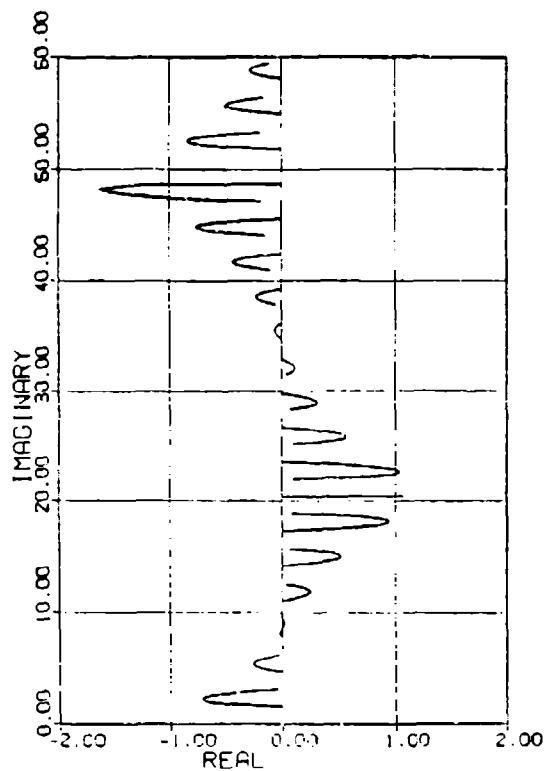


Figure 9 Feedback System with First Order Actuator



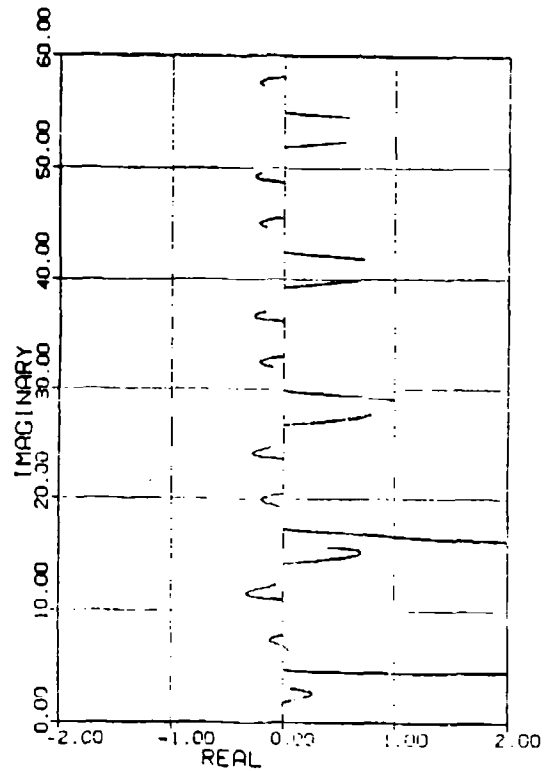
FIXED-FREE CABLE FEEDING BACK VELOCITY
TO FORCE - 1ST ORDER $\tau=0.1$

Figure 10



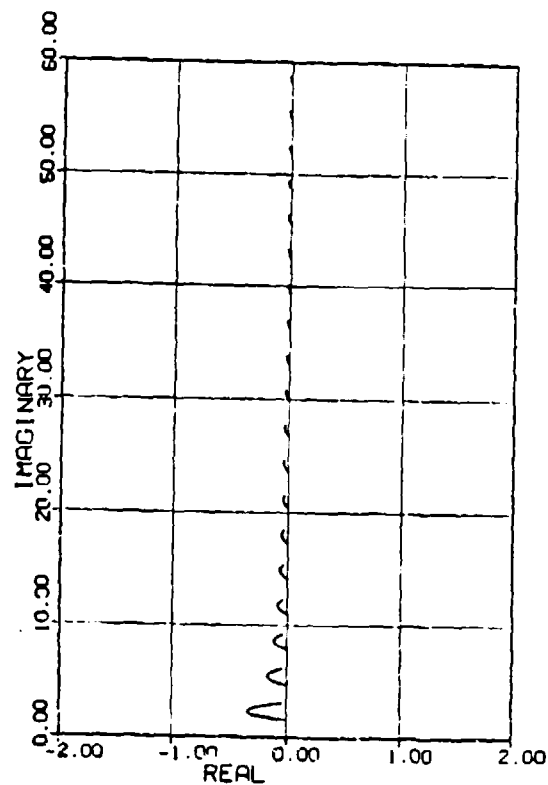
FIXED-FREE CABLE FEEDING BACK VELOCITY
TO FORCE -DELAY & 1ST ORDER T=0.1

Figure 13



FIXED-FREE CABLE FEEDING BACK VELOCITY
TO FORCE -DELAY & 1ST ORDER T=0.5

Figure 14



FIXED-FREE CABLE FEEDING BACK VELOCITY
10 FORCE - 1ST ORDER $I=0.5$

Figure 11

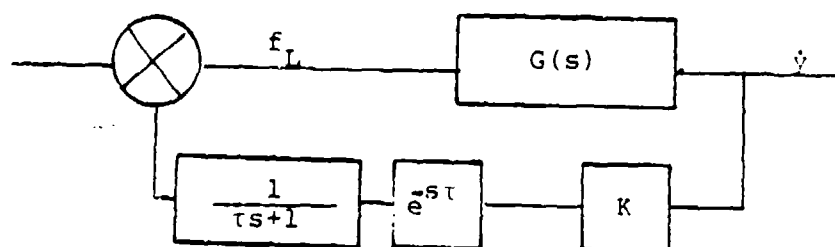
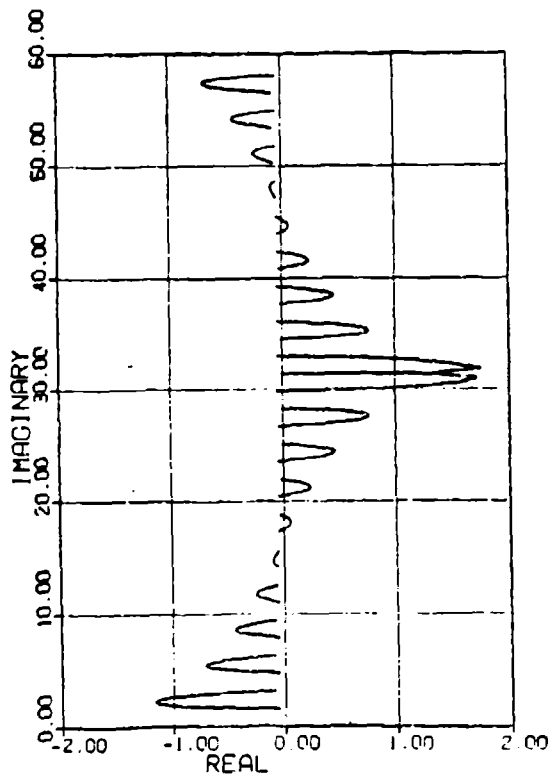


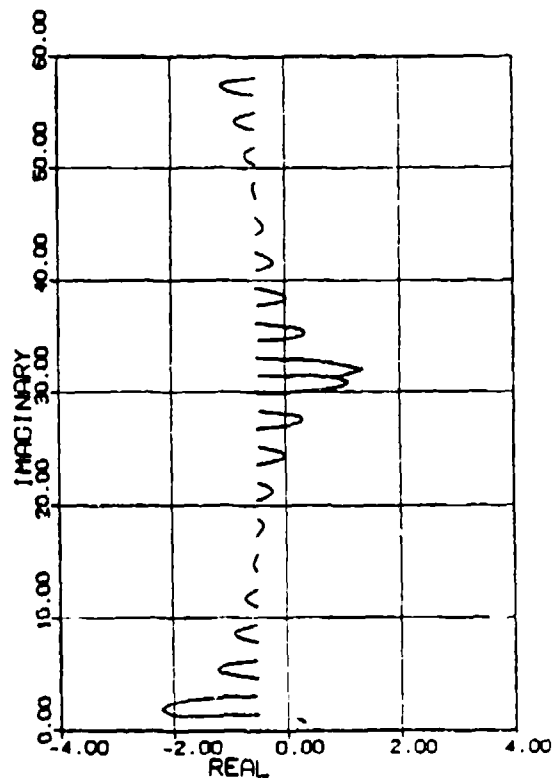
Figure 12 Feedback System with First Order
Actuator and Delay



FIXED-FREE CABLE FEEDING BACK VELOCITY

DAMPING C = 0.1 - DELAY T = 0.1

Figure 15



FIXED-FREE CABLE FEEDING BACK VELOCITY

DAMPING C = 1.0 - DELAY T = 0.1

Figure 16

Program Listing

```

C      THIS ROUTINE SOLVES A SYSTEM OF TRANSCENDENTAL NONLINEAR EQUATIONS
C
C      IT USES IMSL ROUTINE ZSCNT
C      THE VARIABLES USED ARE: PAR(1) = G = GAIN, PAR(2) = TIME DELAY
C      X(1) = R = REAL PART OF ROOT, X(2) = W = IMAGINARY PART OF ROOT
C      S = COMPLEX (R,W), K = NO. OF ROOTS, NR = NO. OF POINTS PER ROOT
C      THE PROGRAM READS FROM DATA FILE 3 AND WRITES TO FILE 4 .
C      CHAR = CHARACTERISTIC EQUATION (THIS CASE FIX-FREE CABLE W/DELAY
C      COMPLEX SH,Z,CH,SI,CO,S,CHAR,TS
C      EXTERNAL FCN
C      DIMENSION X(50),F(50),PAR(50),WK(50)
C      READ IN TIME DELAY
C      READ (3,*) PAR(2)
C      READ ONE AT A TIME EACH OF 19 ROOTS, INITIALIZE GAIN = 0
C      DO 30 K=1,19
C      PAR(1)=0.0
C      READ (3,*) X(1),X(2)
C      WRITE (4,5) X(1),X(2),PAR(2)
5      FORMAT (10X,33HSTART REAL IMAGIN. AND TIME DELAY,/,3E15.4,/)
C      WRITE (4,2)
2      FORMAT(6X,7HREAL S,9X,7HIMAG. S,7X,10HNORM ERROR,5X,4HGAIN)
C      8 SIGNIFICANT FIGURES, TWO EQUATIONS (I.E. REAL AND IMAGINARY)
C      NSIG = 8
C      N = 2
C      ITMAX = 200
C      KNN = N
C      SOLVE EQUATIONS FOR 100 POINTS FOR EACH ROOT
C      DO 20 NR = 1,100
C      CALL ZSCNT (FCN,NSIG,N,ITMAX,PAR,X,FNORM,WK,IER)
C      WRITE(4,1) (X(I), I=1,KNN), FNORM, PAR(1)
1      FORMAT (4E15.4)
C      INCREMENT THE GAIN SLOWLY SO THE SOLVER TO FOLLOW THE ROOT LOCUS
20     PAR(1) = 1.04*(PAR(1)+0.02)
C      WRITE(4,4)
4      FORMAT (1H1)

```

```

30  CONTINUE
    STOP
    END
    SUBROUTINE FCN (X,F,N,PAR)
    COMPLEX SH,Z,CH,SI,CO,S,CHAR,TS
    DIMENSION X(N),F(N),PAR(1)
C   ABREVIATE SIN, COS, SINH, AND COSH
    SH(Z)=(CEXP(Z)-CEXP(-Z))/(2.0,0.0)
    CH(Z)=(CEXP(Z)+CEXP(-Z))/(2.0,0.0)
    SI(Z)=CSIN(Z)
    CO(Z)=CCOS(Z)
    R=X(1)
    W=X(2)
    G=PAR(1)
    S=CMPLX (R,W)
    TS = S * PAR(2)
C   THE CHARACTERISTIC EQUATION GOES HERE
    CHAR=CH(S)+G*(CH(TS)-SH(TS))*SH(S)
    F(1)=REAL(CHAR)
    F(2)=AIMAG(CHAR)
    RETURN
    END

```

Data Input File

```

0.1
0.0  1.570796
0.0  4.712389
0.0  7.853982
0.0 10.995574

```

Output For One Root

START REAL IMAGIN. AND TIME DELAY

```

0.0          0.1571E+01    0.1000E+00

```

REAL S	IMAG. S	NORM ERROR	GAIN
0.0	0.1571E+01	0.9858E-13	0.0
-0.2059E-01	0.1574E+01	0.5090E-12	0.2080E-01
-0.4211E-01	0.1578E+01	0.1089E-13	0.4243E-01
-0.6462E-01	0.1581E+01	0.2269E-11	0.6493E-01
-0.8820E-01	0.1585E+01	0.9173E-12	0.8833E-01
-0.1129E+00	0.1589E+01	0.2791E-12	0.1127E+00
-0.1389E+00	0.1593E+01	0.9437E-13	0.1380E+00
-0.1663E+00	0.1598E+01	0.1360E-11	0.1643E+00
-0.1952E+00	0.1603E+01	0.2402E-11	0.1917E+00
-0.2257E+00	0.1609E+01	0.1796E-11	0.2201E+00
-0.2580E+00	0.1615E+01	0.9998E-13	0.2497E+00
-0.2924E+00	0.1621E+01	0.1628E-11	0.2805E+00
-0.3291E+00	0.1629E+01	0.1374E-11	0.3125E+00
-0.3685E+00	0.1638E+01	0.3695E-12	0.3458E+00